

Research Article

Hydrochemistry and Water Quality Index for Sustainable Drinking Water and Irrigation Management of Mbankomo (Center, Cameroon)

Achille Basile Anaba Onana^{*}, Derrick Kengni Kengmo, Alix Audrey Nga Onana, Jules Remy Ndam Ngoupayou

Geosciences of Superficial Formations and Applications Laboratory, Department of Earth Sciences, Faculty of Science, University of Yaounde I, Yaounde, Cameroon

Abstract

Hydrochemistry is the study of chemical properties and processes that occur in water, including the interactions between water and the surrounding environment. To understanding the chemical composition of water and assess their suitability for drinking and irrigation purpose, water samples were collected of Mbankomo at 10 locations during rainy seasons. From these samples, anions and cations were separated by high performance liquid chromatography (HPLC) using a Dionex ICS-1100 with 0.45 μm diameter. From the findings, it is clear that surface water has an average pH of 5.63 while, groundwater has an arithmetic mean pH of 5.94, with a range between 5.00 and 6.64. These data indicate that the water remains acidic. From the values of TDS (Total Dissolved Solid) (average value of 26.65 mg/l. in surface water; 27.30 to 118.38 mg/l, in groundwater) water samples in the study area are considered fresh (TDS < 1000 mg/l). Water in the research area acquires mineralization through a variety of natural geochemical processes, such as weathering, dissolution, ion exchange processes, and human activity. WQI (Water Quality Index), based on 14 major parameters indicate that water of study area are good to excellent and can use for drinking, irrigation and industry. The water of study area is suitable for irrigation for almost all types of crops with a possibility of limited sodium hazards.

Keywords

Hydrochemistry, Water Quality, Irrigation Management, Mbankomo, Cameroon

1. Introduction

Access to clean and safe drinking water is a fundamental human right and a critical component of sustainable development. Water on Earth is predominantly saline, comprising approximately 97% salt water, of which only 3% is fresh water. Approximately 67% of this freshwater is stored in ice caps and glaciers, 30% exists as groundwater, and the re-

maining 3% is accessible as surface water [1-2]. Water stands as the quintessence of all vital and fundamental resources for the sustenance and survival of all life on Earth. The availability and quality of water resources are known to have immediate and long-term impacts on society's worldwide [3]. In arid and semi-arid regions, this natural resource is a pivotal

^{*}Corresponding author: anabuzza@yahoo.fr (Achille Basile Anaba Onana)

Received: 3 May 2025; **Accepted:** 3 June 2025; **Published:** 30 June 2025



Copyright: © The Author(s), 2025. Published by Science Publishing Group. This is an **Open Access** article, distributed under the terms of the Creative Commons Attribution 4.0 License (<http://creativecommons.org/licenses/by/4.0/>), which permits unrestricted use, distribution and reproduction in any medium, provided the original work is properly cited.

because it can be utilized for both drinking and irrigation [4, 5]. In recent years, there has been an increase in the over-exploitation and contamination of surface water and groundwater in many areas, which has had serious consequences and has caused widespread public concern [6-8]. Geochemical research on water has been demonstrated to facilitate enhanced recognition of water quality and the influences of environmental change [9-12]. These influences encompass processes such as rock weathering, evaporation, and the impact of human activities. The chemical characteristics of water are of pivotal importance when evaluating and categorizing water quality. As posited by [13-16], several factors influence water quality. These include the geology of the area, the extent of chemical weathering of different rock types, the quality of the recharge water, the interactions between water and rock and anthropogenic activities. In regions like Mbankomo, located in the Center Region of Cameroon,

the interplay between hydrochemistry and water quality significantly influences both public health and agricultural productivity. As urbanization and population growth exert increasing pressure on water resources, understanding the chemical composition of water sources becomes essential for effective management and policy-making. This article explores the hydrochemical characteristics of water in Mbankomo, assessing its suitability for drinking and irrigation purposes. By employing a WQI framework, we aim to provide a comprehensive evaluation of water quality, highlighting the implications for sustainable water management practices. Through this analysis, we seek to contribute valuable insights that can guide local authorities and stakeholders in ensuring the availability of safe drinking water and optimizing irrigation strategies, ultimately fostering a healthier and more resilient community.

2. Materials and Methods

2.1. Study Area

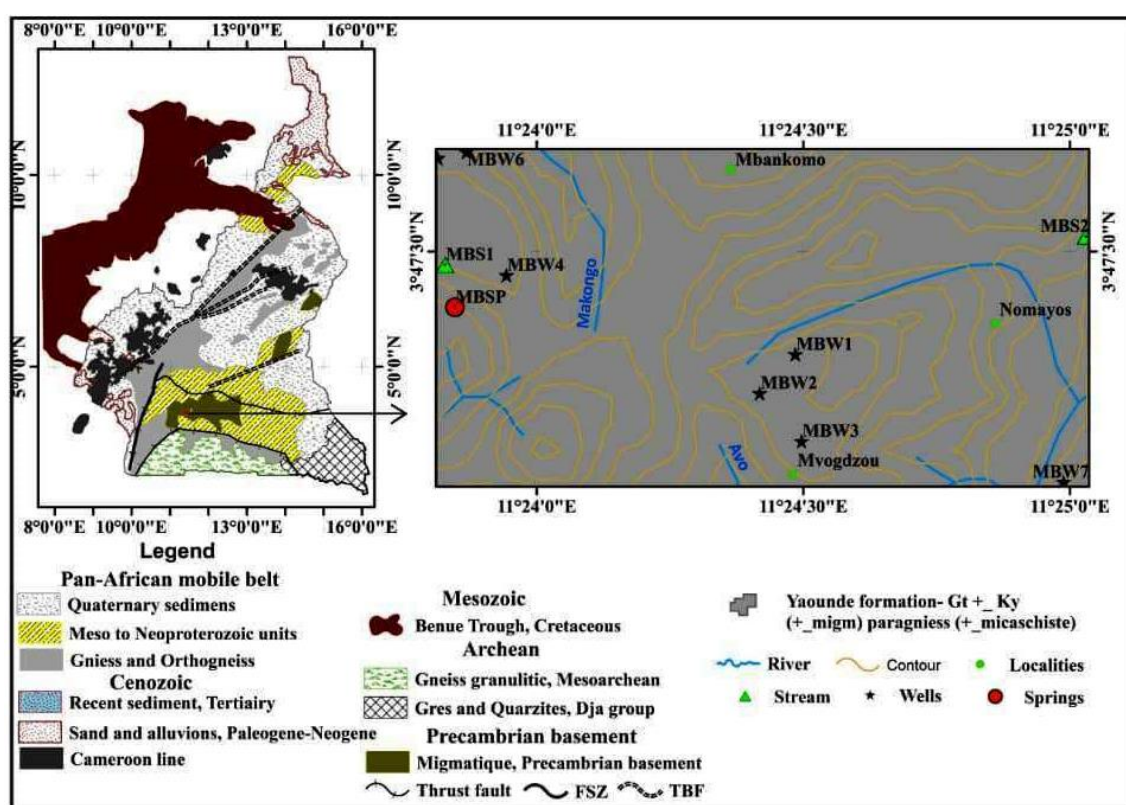


Figure 1. Geologic map of the study area with water sample.

The commune of Mbankomo, situated in the Centre Region of Cameroon within the Mefou-et-Akono department, covers an area of 1,300km² (approximately 22 km from Yaounde). It is situated between 11°13' and 11°39' east longitude and 3°37'

and 3°57' north latitude, comprising 66 villages. The average altitude of the commune is 787 meters, and its population density is 46 inhabitants per km² (Figure 1). From a geological perspective, the Yaounde region is located in the mobile

zone of Africa, more precisely in the Pan-African chain aged 540 to 600 million years, as evidenced by the works of [17-20]. The area under consideration extends to a total of more than 7000 km² [21]. From a regional perspective, the area can be categorised into two distinct lithological groups: one characterised by weak metamorphism, comprising the Ayos, Bengbis, and Yokadouma series, and the other exhibiting medium to high metamorphism, constituted by the Yaoundé and Nanga-Eboko series. The latter is composed of gneiss, migmatites, micaschists, amphibolites, and calcic silicate rocks. From a hydrogeological perspective, the region under study is part of crystalline bedrock, which is essentially composed of two aquifers: a deeper discontinuous aquifer connected to major cracks and an upper aquifer situated in the granular worn bedrock [22]. The upper aquifer is characterised by its nearly isotropic nature, with a depth range of 8 to 20 metres. Water discovered beyond 20 meters in the lower aquifer is anisotropic. The saprolite voids that contain the water of the upper aquifer have a poor permeability yet a considerable capacity to store groundwater [23]. The water in the lower aquifer is located within the basement bills and fissures that were created by weathering processes and the passage of altered deep veins across the bedrock [24-27].

2.2. Water Sampling

In order to ascertain the hydrogeochemical characteristics of the water, a total of ten (10) samples were collected. These comprised one spring, 7 excavated wells tapping into the shallow aquifer (2-12 m), and two surface water samples. The samples were gathered in October 2022 (rainy season). The selection of sampling locations was influenced by factors such as the owner's consent, accessibility, and the water table conditions of the dug wells. A Garmin 64S GPS was employed to record the geographical coordinates at each sampling site. In order to obtain a sample of water from the aquifer which was representative of the total, samples were collected from the excavated wells between 7am and 10am, i.e. when residential water extraction is at its peak. In-situ parameters such as pH, electrical conductivity (EC), and temperature (T) were measured using HANNA multimeters. The pH meter was calibrated using different buffer solutions at pH 4.0, 7.0, and 12.0, while the electrode of the EC meter was calibrated with a 0.01 M KCl standard (1413 μ S.cm⁻¹). The collection of a river sample was achieved by submerging the sampling bottles in the centre of the channel at a depth of approximately 30 cm, in areas exhibiting the highest flow velocity [28-31]. This approach ensures effective homogenisation of solid particles and dissolved components [32]. The collection of groundwater samples was undertaken using a variety of methods, direct immersion of a bottle in relation to springs, and, in the case of wells, the repeated rinsing of the bucket with sample water prior to filling. In accordance with the recommended procedures outlined by [33], water samples were collected in sanitized 500 ml polyethylene bottles and

kept in a chiller at 4 °C until examination in the laboratory. A small quantity of concentrated HNO₃ was added to the samples intended for cations analysis. Prior to filling, the sample water was used to rinse each bottle three times.

2.3. Data Treatment

2.3.1. Laboratory Analysis

Once at the laboratory, the samples were filtered by the frontal filtration method using an electric vacuum pump. This filtration unit is equipped with a cellulose millipore filter (NALGENE filter) with a porosity of 0.4 μ m, which was previously dried in an oven at 105 °C for 3 hours. This procedure was used to obtain the TSS and the filtrate for chemical analysis. Anions and cations were separated by high performance liquid chromatography (HPLC) using a Dionex ICS-1100 with 0.45 μ m diameter. The concentrations of Ca²⁺, Mg²⁺ and SO₄²⁻ were measured using the EDTA (Ethylene Diamine Tetraacetic Acid) titration method with an error of $\pm 1\%$, $\pm 1\%$ and $\pm 0.5\%$ respectively. K⁺ and Na⁺ concentrations were determined by FAME atomic absorption spectrophotometry with an accuracy of 0.1 mg/L. Anion concentrations were determined by argentometric titration with a relative error of $\pm 1\%$. All analyses were performed according to the standard procedures proposed by the American Public Health Association [33-37].

2.3.2. Identification of the Factors Controlling Water Quality in the Study Area

The chemical parameters obtained were utilised to calculate the choro-alkaline indices (CAI 1 and CAI 2, [38-40]), The chloro-alkaline indices were determined using the aforementioned formula.

$$CAI - 1 = Cl^- - (Na^+ + K^+) / Cl^- \quad (1)$$

$$CAI - 2 = Cl^- - (Na^+ + K^+) / (SO_4^{2-} + HCO_3^- + NO_3^-) \quad (2)$$

The relation between the concentrations of calcium (Ca²⁺), magnesium (Mg²⁺), bicarbonate (HCO₃⁻) and sulphate (SO₄²⁻) ions, expressed as a function of the concentrations of sodium (Na⁺) and potassium (K⁺) ions, and chlorine (Cl⁻) ions, has been utilized to elucidate the role of the cation exchange mechanism in the process of groundwater mineralization. In the event of the two parameters exhibiting a linear connection with a slope of -1, it is confirmed that there is cation exchange [41, 42].

The Gibbs model is a technique for determining and comprehending the origin of groundwater mineralisation between precipitation, evaporation, and water-rock interaction [43-45, 35, 36]. The Gibbs value and the diagram have been obtained using Diagram software, which uses the equation below (Eq. 3).

$$\text{TDS} = f(\text{Na}^+ / \text{Na}^+ + \text{Ca}^{2+}) \text{ and } \text{TDS} = f(\text{Cl}^- / \text{Cl}^- + \text{HCO}_3^-) \quad (3)$$

2.3.3. Water Quality Index

(i) Water Quality Assessment for Drinking

The Water Quality Index (WQI) is an effective and straightforward mathematical tool used to evaluate the overall quality of groundwater. It takes into account various criteria that determine its suitability for drinking and irrigation purposes [46, 47]. In this study, the water analyzed characteristics, which were taken into consideration for the calculation of this indice are pH, EC, TSS, T °C, Na⁺, K⁺, Mg²⁺, Ca²⁺, Cl⁻, NO₃⁻, SO₄²⁻, HCO₃⁻, F, PO₄³⁻. This calculation of this parameter is divided into four stages [35, 48-51].

Step 1: The initial step involves assigning a weight (wi) to each selected parameter for calculating the Water Quality Index (WQI), based on its significance for water quality and its impact on human health. The assigned weights range from 1 to 5, with a value of 1 indicating low importance (e.g., HCO₃⁻) and a value of 5 representing the highest priority parameters for overall water quality assessment (such as TDS, NO₃⁻, F⁻, etc.).

Step 2: In this stage, the relative weight of each parameter is determined (Eq. (4)).

$$W_i = \frac{k}{s_i} \quad (4)$$

where Wi denotes the relative weight, n represents the total number of parameters, and wi is the assigned weight for each individual parameter.

k is proportionality constant given by the relationship [52].

$$k = \frac{1}{\sum_{i=1}^n \left(\frac{1}{s_i}\right)} \quad (5)$$

Step 3: This step involves calculating the quality rating scale (qi) for each parameter (Eq. (6)).

$$q_i = \frac{C_i}{S_i} * 100 \quad (6)$$

where qi represents the quality rating scale, Si is the drinking water standard [53] for each chemical parameter, and Ci is the observed value of each chemical parameter in mg/L.

Step 4: In this final step, the overall Water Quality Index (WQI) was then calculated by the following formula (Eq. (7)):

$$\text{WQI} = \frac{q_i w_i}{\sum w_i} \quad (7)$$

Finally, the classification of water types is determined based on the WQI value, as outlined in Table 1 [54-56].

The other water quality indices used are pollution and agricultural indices from equations proposed by [57, 58] (Eqs. 8 & 9). These indices were calculated using sample's anion

concentration ratios.

$$\% \text{pollution} = \frac{[\text{Cl}^-] + [\text{SO}_4^{2-}] + [\text{NO}_3^-]}{[\text{Cl}^-] + [\text{SO}_4^{2-}] + [\text{NO}_3^-] + [\text{HCO}_3^-]} \quad (8)$$

$$\% \text{agriculture} = \frac{[\text{SO}_4^{2-}] + [\text{NO}_3^-]}{[\text{Cl}^-] + [\text{SO}_4^{2-}] + [\text{NO}_3^-]} \quad (9)$$

Table 1. Classification of water quality based on WQI value [122, 123].

Rank	WQI	Water quality	Possible Use
1	0 - 25	Excellent	Potable water. irrigation and industry
2	25 - 50	Good	Potable water. irrigation and industry
3	50 - 75	Poor	Irrigation and industry
4	75 - 100	Very poor	Irrigation
5	> 100	Non-drinkable water	Suitable treatment before use

(ii) Irrigation Water Quality Assessment

The quality of the water used for irrigation is an important indicator of the quality of the crop and its effect on soil characteristics. Achieving superior crop production necessitates the use of water that is both nutrient-rich and free from any pathogens. The adverse effects of water quality on crop yield are attributable to toxicity and nutrient inadequacy. A number of factors must be taken into account when determining the suitability of Deepor Beel water for irrigation. These are outlined below, with the relevant ionic concentration levels in meq/L of the corresponding elements shown inside the square bracket.

1. Sodium adsorption ratio (SAR)

SAR (Eq. 10) is measured as sodium concentration with respect to calcium and magnesium. This essentially determines the measure of sodium hazard [59].

$$\text{SAR} = \frac{[\text{Na}^+]}{\sqrt{\frac{[\text{Ca}^{2+}] + [\text{Mg}^{2+}]}{2}}} \quad (10)$$

2. Kelly's ratio (KR)

KR (Eq. 11) is a further tool for measuring sodium hazard, which is expressed as a fraction of sodium to calcium and magnesium concentrations [60].

$$\text{KR} = \frac{[\text{Na}^+]}{[\text{Ca}^{2+}] + [\text{Mg}^{2+}]} \quad (11)$$

3. Soluble sodium percentage (SSP)

Sodium, when present in excess, can hinder plant growth by reducing soil permeability. Therefore, assessment of SSP

(Eq. 12) is critical [61].

$$SSP = \frac{[Na^+] + [K^+]}{[Na^+] + [K^+] + [Ca^{2+}] + [Mg^{2+}]} \times 100 \quad (12)$$

4. Residual sodium carbonate, RSC

The study [62] developed an equation to quantify RSC in water with high HCO_3^- , because they tend to precipitate as carbonates of Ca^{2+} and Mg^{2+} . The equation is as follows:

$$RSC = (HCO_3^- + CO_3^{2-}) - (Ca^{2+} + Mg^{2+}) \quad (13)$$

5. Magnesium adsorption ratio (MAR)

Excess magnesium in the water can significantly disrupt crop growth by making the water more alkaline. As outlined in equation 15, the MAR model is a useful tool for assessing the potential magnesium hazard to crop yield [63].

$$MAR = \left\{ \frac{[Mg^{2+}]}{[Ca^{2+}] + [Mg^{2+}]} \right\} \times 100 \quad (14)$$

6. Potential Salinity

The potential risks associated with high salt concentrations (Cl^- and SO_4^{2-}) in irrigation water were assessed utilising the PS, calculated according to the following equation (Eq. 15) [64]:

$$PS = Cl^- + \frac{SO_4^{2-}}{2} \quad (15)$$

3. Results and Discussion

3.1. Physicochemical Parameter of Water

The physico-chemical analysis of the water samples is summarized in Table 2. The data demonstrate that the average of temperature of surface water is 22.95 °C and for groundwater this parameter varied from 24.20 to 24.90 °C, with an average of 24.55 °C. The groundwater temperature is shown to be significantly higher than the average of the atmospheric temperature, indicating a strong degree of infiltration into the aquifer within the study area. Surface water has an average pH of 5.63. In contrast, groundwater has an arithmetic mean pH of 5.94, with a range between 5.00 and 6.64. The US Environmental Protection Agency (EPA) considers pH to be a secondary guideline for drinking water and recommends a pH range of 6.5 to 8.5 for drinking water [65]. The values obtained in this study are therefore outside this range. The study indicates that the water remains acidic, with a pH of less than 7, which aligns with findings from other researchers who have reported similar results in the water of Yaoundé [66, 67], [68] in the Ndop plain of North west Cameroon; [69] in Mbal-mayo's groundwater, as well as [42] in the Mayo Bocki watershed in North Cameroon; [70] in Ngaoundere Cameroon;

[71] in central Cameroon. [72-74] suggest that the observed acidity is influenced by several factors, including the presence of acids from organic matter decomposition [32, 75] and the siliceous composition of the basement in the central region. The presence of acidity in the water can be attributed to the leaching process that occurs at the landfill sites in the locality. Given the nature of the landfill site, which contains a variety of waste materials, including lead-acid batteries and plastic stabilisers from multiple sources, there is a high probability of acid leaching from these wastes. This process has the potential to result in the entry of these materials into the Mbankomo ecosystem, leading to a significant decrease in pH levels [76]. In surface water, total dissolved solids (TDS) have an average value of 26.65 mg/l. In the groundwater, the TDS values range from 27.30 to 118.38 mg/l, with an arithmetic mean of 51.44 mg/l. Based on [77] classification, all water samples in the study area are considered fresh ($TDS < 1000$ mg/l). The mean value of electrical conductivity in surface water is 38.65 $\mu S/cm$. Conversely, groundwater electrical conductivity varies from 42.10 to 181.38 $\mu S/cm$, with an average of 78.92 $\mu S/cm$. The mineralization levels in surface water range from low to medium, while groundwater exhibits extremely weak mineralization. All water samples have electrical conductivity below the acceptable limit stipulated by the World Health Organization (WHO). The electrical conductivity of surface water averaged at 38.65 $\mu S/cm$, while in groundwater it ranged from 42.10 to 181.38 $\mu S/cm$, with an average of 78.92 $\mu S/cm$. The analysis indicates that all the water samples in the study area exhibit low to medium levels of mineralization, which are within the limits authorized by the World Health Organization (WHO). The order of abundance of cations and anions concentrations is as follow $Ca^{2+} > Na^+ > K^+ > Mg^{2+} > NH_4^+$ and $SO_4^{2-} > NO_3^- > Cl^- > HCO_3^- > F^- > PO_4^{3-}$. The average TDS increased from one to almost double from surface water (26.65 mg/l) to groundwater (51.44 mg/l). Conversely, the mean relative concentrations of dissolved ions other than Cl^- , SO_4^{2-} , HCO_3^- and F^- exhibited an increase from groundwater to surface water (Figure 2). This phenomenon can be attributed to the collection of samples during the rainy season, a period of heightened stream water activity. The leaching of soil by stream water is a plausible cause of the elevated ion concentrations observed in surface water relative to groundwater, particularly given the comparatively higher water flow rates characteristic of this season. The relatively elevated TDS in groundwater is indicative of the impact of unconsolidated sediments and crystalline rocks on the chemical enrichment of water as it percolates through the under saturated zone (or flows through the aquifer) [78]. The low concentrations of major ions in groundwater are indicative of the weak water-rock interactions in the granitic basement, the short residence time, the shallow nature of the aquifer and its acidic nature) [79].

Table 2. Physical and chemical parameters of water of Mbankomo (Cameroon).

Water type	CODE	T (°C)	pH	EC (µS/cm)	MES (mg/l)	TDS (mg/l)	Na+ (mg/l)	K+ (mg/l)	Mg2+ (mg/l)
Surface water	MBS1	23.60	6.37	46.30	1.55	31.85	0.85	0.67	0.44
	MBS2	22.30	4.90	31.00	1.97	21.45	1.22	0.77	0.61
	Mean	22.95	5.63	38.65	1.76	26.65	1.03	0.72	0.52
	MBSP	24.70	6.64	45.70	2.03	118.38	0.73	0.53	0.27
	MBW1	24.60	6.50	181.38	0.80	81.90	0.15	0.06	0.06
Groundwater	MBW2	24.30	6.38	124.90	1.50	55.90	0.14	0.05	0.06
	MBW3	24.90	5.55	86.20	0.96	31.20	0.14	0.06	0.07
	MBW4	24.50	5.58	47.90	0.88	35.75	0.13	0.05	0.09
	MBW5	24.20	5.50	55.30	3.90	31.20	0.15	0.05	0.09
	MBW6	24.30	5.00	47.90	2.36	27.30	0.19	0.08	0.11
	MBW7	24.90	6.41	42.10	2.70	29.90	1.15	1.04	0.73
	Min	24.20	5.00	42.10	0.80	27.30	0.13	0.05	0.06
	Max	24.90	6.64	181.38	3.90	118.38	1.15	1.04	0.73
	Mean	24.55	5.94	78.92	1.89	51.44	0.35	0.24	0.19
Water type	CODE	Ca ²⁺ (mg/l)	NH ⁴⁺ (mg/l)	Cl ⁻ (mg/l)	NO ₃ ⁻ (mg/l)	SO ₄ ²⁻ (mg/l)	HCO ₃ ⁻ (mg/l)	F ⁻ (mg/l)	PO ₄ ³⁻ (mg/l)
Surface water	MBS1	3.67	0.05	9.64	26.52	18.50	0.99	0.20	0.08
	MBS2	1.83	0.29	15.52	102.07	11.65	0.99	0.55	0.00
	Mean	2.75	0.17	12.58	64.29	15.07	0.99	0.37	0.04
	MBSP	3.09	0.07	11.45	55.29	18.93	0.36	0.41	0.03
	MBW1	0.17	0.03	4.35	23.66	83.66	0.60	1.06	0.01
Groundwater	MBW2	0.14	0.03	15.87	33.52	71.06	0.95	0.93	0.02
	MBW3	0.13	0.02	29.97	116.74	339.24	1.58	1.40	0.03
	MBW4	0.18	0.02	22.51	89.73	194.87	1.98	1.07	0.04
	MBW5	0.21	0.04	14.10	44.77	35.72	6.23	0.41	0.01
	MBW6	0.32	0.06	8.61	44.81	18.50	0.90	3.00	0.03
	MBW7	1.53	0.03	21.74	61.15	10.94	0.88	0.86	0.02
	Min	0.13	0.02	4.35	23.66	10.94	0.36	0.30	0.01
	Max	3.09	0.07	29.97	116.74	339.24	6.23	1.38	0.04
	Mean	0.72	0.03	16.08	58.71	96.61	1.68	0.80	0.02

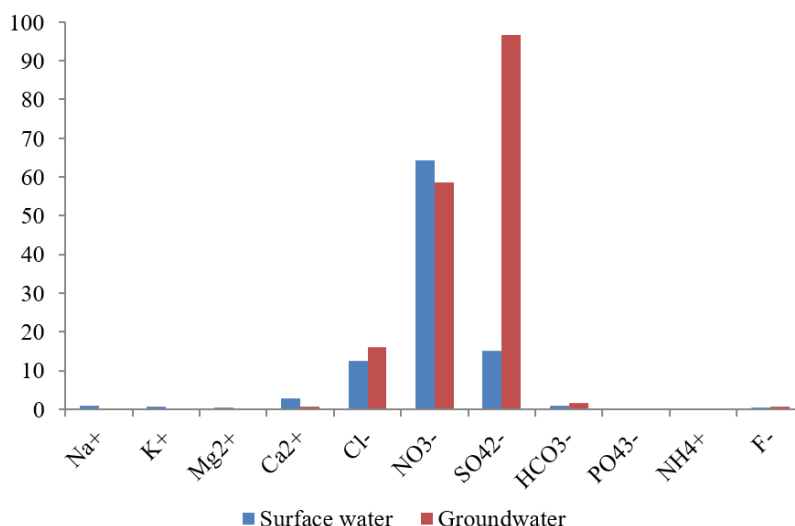


Figure 2. Mean relative concentrations of ions in water of the study area.

3.2. Hydro Chemical Facies of Water

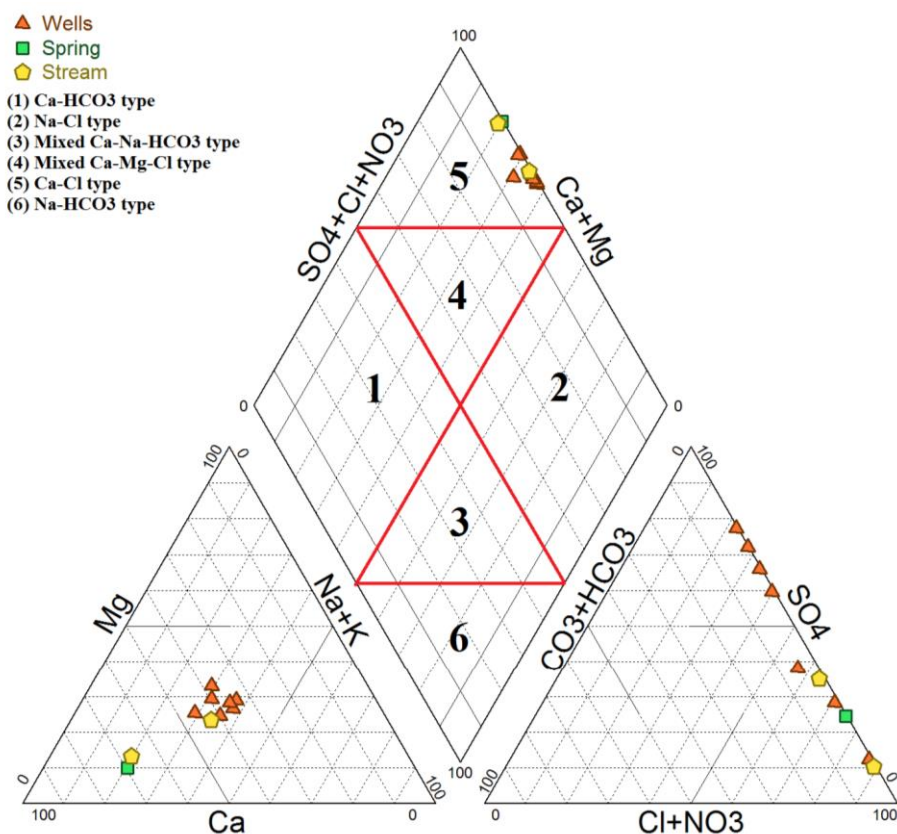


Figure 3. Water facies showing of Mbankomo.

The cations and anions were plotted on a trilinear diagram proposed by [80] to analyze the water facies (Figure 3). As this diagram demonstrate, it is possible to facilitate comprehension of the geochemical evolution of water in general. The

diagram illustrates only one facies: Ca-Mg-Cl-SO₄. This facies exhibited evidence of a mixing process involving two distinct elements: firstly, the presence of anthropogenic pollutants associated with surface contamination sources such as

domestic wastewater and septic tank effluent, and secondly, an ion exchange phenomenon with the surrounding water.

3.3. Geochemical Evolution

The Gibbs diagram (Figure 4) [81] was developed as a means of analysing the various geogenic processes that control the geochemistry of the water in the study area. This diagram has been employed by numerous researchers on multiple occasions to characterize both surface and groundwater [82].

The Gibbs ratios of $\text{Na}^+ + \text{K}^+ / (\text{Na}^+ + \text{K}^+ + \text{Ca}^{2+})$ and $\text{Cl}^- / (\text{Cl}^- + \text{HCO}_3^-)$ plotted against Total Dissolved Solids (TDS) were utilized to identify the dominant environmental controls on water chemistry. All of the samples analyzed were found to fall within the range of dominance of rock weathering.

stituents in surface water and groundwater is principally attributable to rock weathering and dissolution processes occurring in soils or aquifer materials along the groundwater flow path. The geology of the study area made of gneiss and migmatite with alteration likely to be responsible for the release of these elements.

The chloroalkaline indices I and II are to be employed for the purpose of ascertaining the chemical reactions in which ion exchange occurs [70, 83, 84]. The study's CAI 1 and CAI 2 results vary from 0.80 to 0.99 and -0.0013 to 0.04, respectively. As illustrated in Table 3, all water samples exhibited a positive response to both CAI-1 and CAI-2. This finding indicates that the sodium (Na) and potassium (K) ions present in the water undergo an exchange process with the magnesium (Mg) and calcium (Ca) ions present in the underlying rocks.

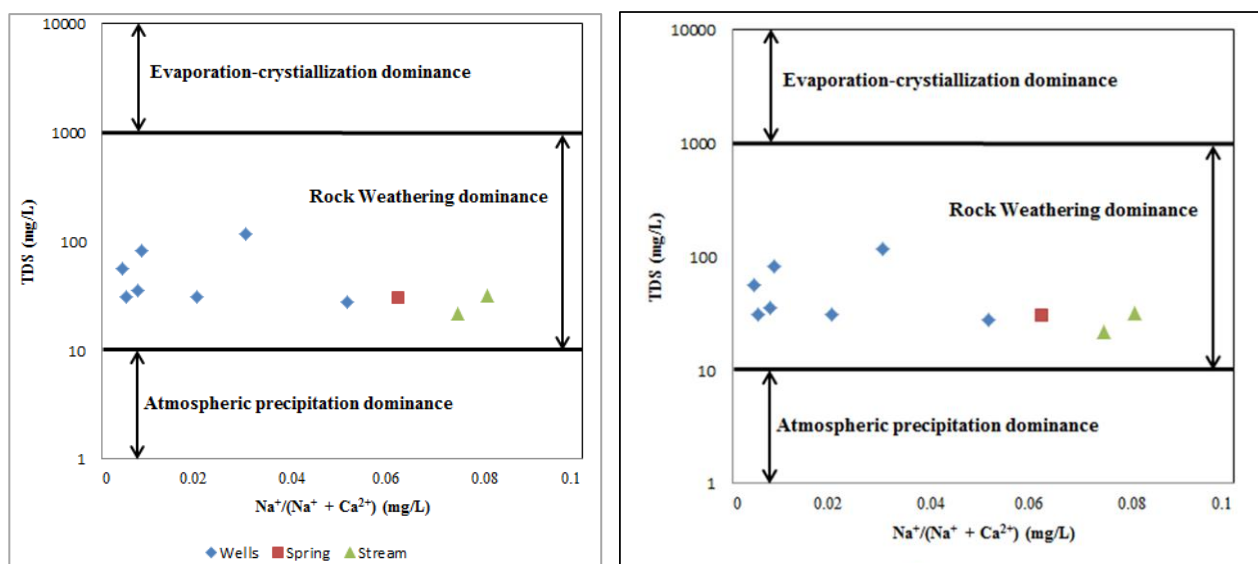


Figure 4. Mechanism governing water chemistry.

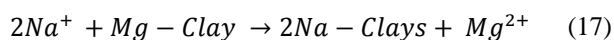
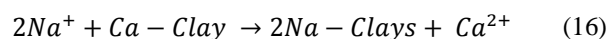
3.4. Origin of Solutes and Hydrochemical Controls

The presence and interactions of ions within water can offer insights into the origins of solutes and the processes that have contributed to its chemical composition, as evidenced by earlier studies [85, 86]. Table 3 shows the correlation coefficients between ionic species in water. The strong positive correlation between NO_3^- and Cl^- indicates their anthropogenic origin [87, 88]. The main potential sources of NO_3^- are the proximity to the numerous shallow pit toilets and the oxidation of organic matter due to the proximity (>15 m) of the shallow water table and the predominance of agriculture, respectively. The correlation coefficient between magnesium and calcium (0.63) is indicative of rock dissolution related to

the residence time of water in the aquifer [89]. The strong correlation between chloride and sulfate ions (0.70) and between potassium and sodium ions (0.98) indicates salinization resulting from latrine proximity or leaching of secondary salts.

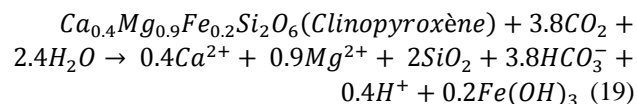
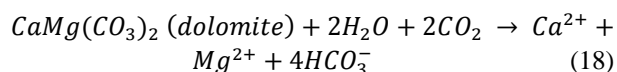
Ionic ratio characterization is necessary to distinguish between the possible origins of the ratios. Additionally, the fundamental hydrogeochemical processes that regulate the aquifer system can be studied using the ions ratio between the principal ions [90-93]. As demonstrated in Figure 5a, the scatter diagram of $\text{Ca}^{2+} + \text{Mg}^{2+}$ as a function of HCO_3^- provides a comprehensive explanation of the sources of Ca^{2+} and Mg^{2+} in the waters of the study area. This analysis offers a more nuanced understanding of the primary source of dissolved solids. The data indicates that the ratio $(\text{Ca}^{2+} + \text{Mg}^{2+})/\text{HCO}_3^-$ for the majority of the samples lies above the

1:1 trend line. This finding suggests that the presence of alkaline earth metals (Ca^{2+} and Mg^{2+}) is predominantly attributable to the weathering of silicates and the dissolution of carbonates, such as dolomite, which is a consequence of the precipitation of calcium carbonate. This confirms that silicate alteration is the main mechanism for the appearance of dissolved salts in water [93-95]. In the study area, the ratio ($\text{Ca}^{2+} + \text{Mg}^{2+}$)/ HCO_3^- varied from 0.18 to 30.12. 90% of water samples have this ratio > 0.5 which suggests that the solutes in the water of the study area are chiefly derived from the alteration processes of silicates, rather than from the dissolution of carbonates [96]. The preponderance of data indicates that the majority of points are concentrated on the Ca^{2+} and Mg^{2+} side, thereby suggesting that the excess calcium and magnesium is derived from alternative processes, such as reverse ion exchange. This is attributable to the fact that if the Ca^{2+} and Mg^{2+} were derived exclusively from the alteration of carbonates and silicates, they would have to be balanced by alkalinity alone [97]. As asserted by [98], the elevated ratio ($\text{Ca}^{2+} + \text{Mg}^{2+}$)/ HCO_3^- indicates that the surplus of Ca^{2+} and Mg^{2+} has been counterbalanced by Cl^- and SO_4^{2-} . Furthermore, evidence has been provided to demonstrate that the ratio ($\text{Ca}^{2+} + \text{Mg}^{2+}$)/ $\text{HCO}_3^- > 0.5$ indicate that a reverse cation exchange process has occurred [99]. The reverse ion exchange processes, which release Ca^{2+} and Mg^{2+} in the groundwater within the watersheds studied, are shown in reactions (16) and (17) [100].



The $\text{Ca}^{2+} + \text{Mg}^{2+}$ vs. $\text{HCO}_3^- + \text{SO}_4^{2-}$ point cloud was utilized to investigate the feasibility of an ion exchange process. In the event of normal ion exchange predominating, the points represented should move towards the $\text{HCO}_3^- + \text{SO}_4^{2-}$ domain. However, if reverse ion exchange does dominate, the shift is towards the $\text{Ca}^{2+} + \text{Mg}^{2+}$ domain [101]. This is due to the increase in Ca^{2+} and Mg^{2+} released from the rocks. The few analysis water samples revealed a correlation with the 1:1 trend line (Figure 5b). This finding suggests the dissolu-

tion of dolomite and silicate minerals in study area, as evidenced by reactions show in equations (18), (19).



In order to assess the impact of silicate and carbonate weathering on groundwater chemistry, the $\text{Mg}^{2+}/\text{Ca}^{2+}$ ratio is also calculated [102]. Figure 5c shows that all the water samples were distributed above the 1:1 trend line, indicating carbonate and silicate minerals rich in magnesium. The ratio of $\text{Mg}^{2+}/\text{Ca}^{2+}$ varies from 0.14 to 0.87 indicating the water-rock reaction mainly dominated by the congruent dissolution of igneous rocks made up of magnesium rich minerals such as ferromagnesian.

The relationship between Na^+ and Cl^- is depicted in figure 5(d), and all the points are on the upper or close side of the trend line, suggesting that the dissolution of halite mineral is not the principal source of Na^+ and Cl^- [92, 93, 103]. Figure 5(e) (Ca^{2+} vs. HCO_3^-) shows that, most of the water samples were below the 1:1 line, in which more HCO_3^- than Ca^{2+} and dissolution of dolomite, clinopyroxene, amphibole, and anorthite happened.

K^+ vs. HCO_3^- shows that all the samples fell below the 1:1 trend line (Figure 5f), indicating higher HCO_3^- than K^+ concentrations, from which the source is mainly biotite due to high temperature.

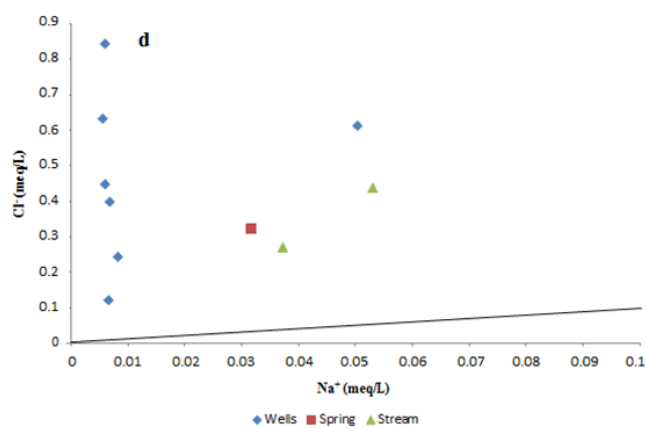
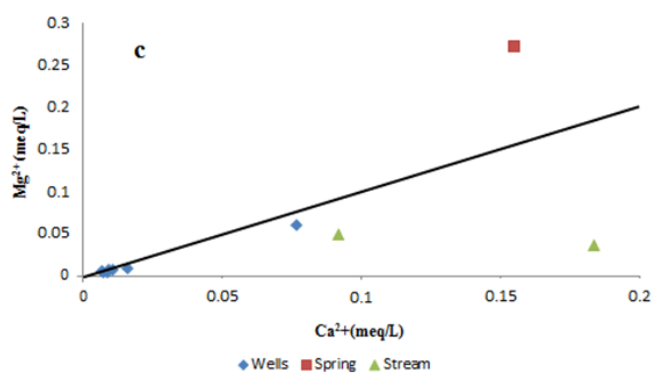
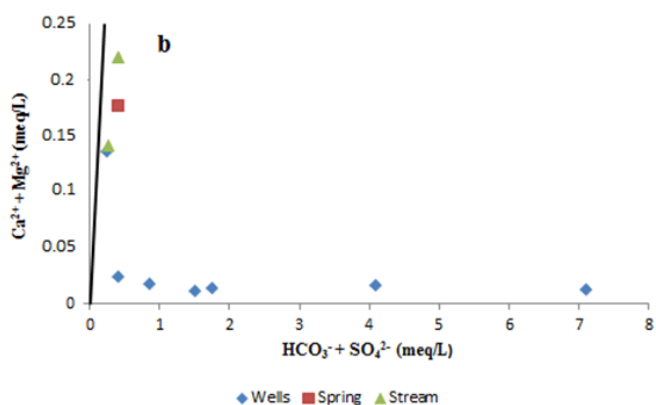
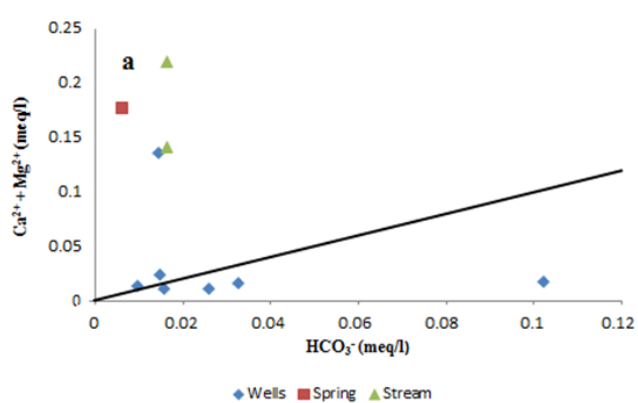
Trends of K^+/Cl^- vs. Cl^- (Figure 5g) revealed that all of water samples in the study area had a K^+/Cl^- ratio < 0.2 , suggesting weathering of K-feldspar is not abundant in the study area.

Plot $\text{Ca}^{2+}/\text{Ca}^{2+} + \text{SO}_4^{2-}$ vs. pH is plotted to represent dissolution of carbonate minerals [104]. In all portions of the study area, all the water samples fell in the area of the Ca^{2+} depletion may have originated from carbonate or silicate sources (Figure 5h).

Table 3. Pearson correlation coefficients of all analyzed water sources.

Parameter	Na^+	K^+	Mg^{2+}	Ca^{2+}	Cl^-	NO_3^-	SO_4^{2-}	HCO_3^-	NH_4^+	F^-	pH	T °C	CE	MES	TDS
Na^+	1.00														
K^+	0.98	1.00													
Mg^{2+}	0.97	0.98	1.00												
Ca^{2+}	0.74	0.73	0.63	1.00											
Cl^-	-0.01	0.03	0.07	-0.26	1.00										
NO_3^-	0.14	0.08	0.14	-0.16	0.80	1.00									

Parameter	Na ⁺	K ⁺	Mg ²⁺	Ca ²⁺	Cl ⁻	NO ₃ ⁻	SO ₄ ²⁻	HCO ₃ ⁻	NH ₄ ⁺	F ⁻	pH	T °C	CE	MES	TDS
SO ₄ ²⁻	-0.53	-0.51	-0.49	-0.48	0.70	0.61	1.00								
HCO ₃ ⁻	-0.33	-0.34	-0.28	-0.35	0.14	0.01	0.05	1.00							
NH ₄ ⁺	0.24	0.22	0.11	0.66	-0.56	-0.37	-0.54	-0.10	1.00						
F ⁻	-0.38	-0.33	-0.30	-0.60	0.62	0.46	0.80	-0.13	-0.81	1.00					
pH	0.08	0.20	0.07	0.36	-0.22	-0.55	-0.16	-0.32	0.13	0.10	1.00				
T °C	-0.49	-0.33	-0.42	-0.33	0.24	-0.14	0.40	0.00	-0.06	0.46	0.48	1.00			
CE	-0.54	-0.52	-0.53	-0.47	-0.28	-0.39	0.24	-0.17	-0.43	0.53	0.42	0.33	1.00		
MES	0.23	0.24	0.27	0.08	-0.12	-0.20	-0.57	0.63	0.33	-0.59	-0.20	-0.10	-0.48	1.00	
TDS	-0.53	-0.51	-0.53	-0.46	-0.29	-0.40	0.24	-0.17	-0.43	0.52	0.42	0.31	1.00	-0.48	1.00



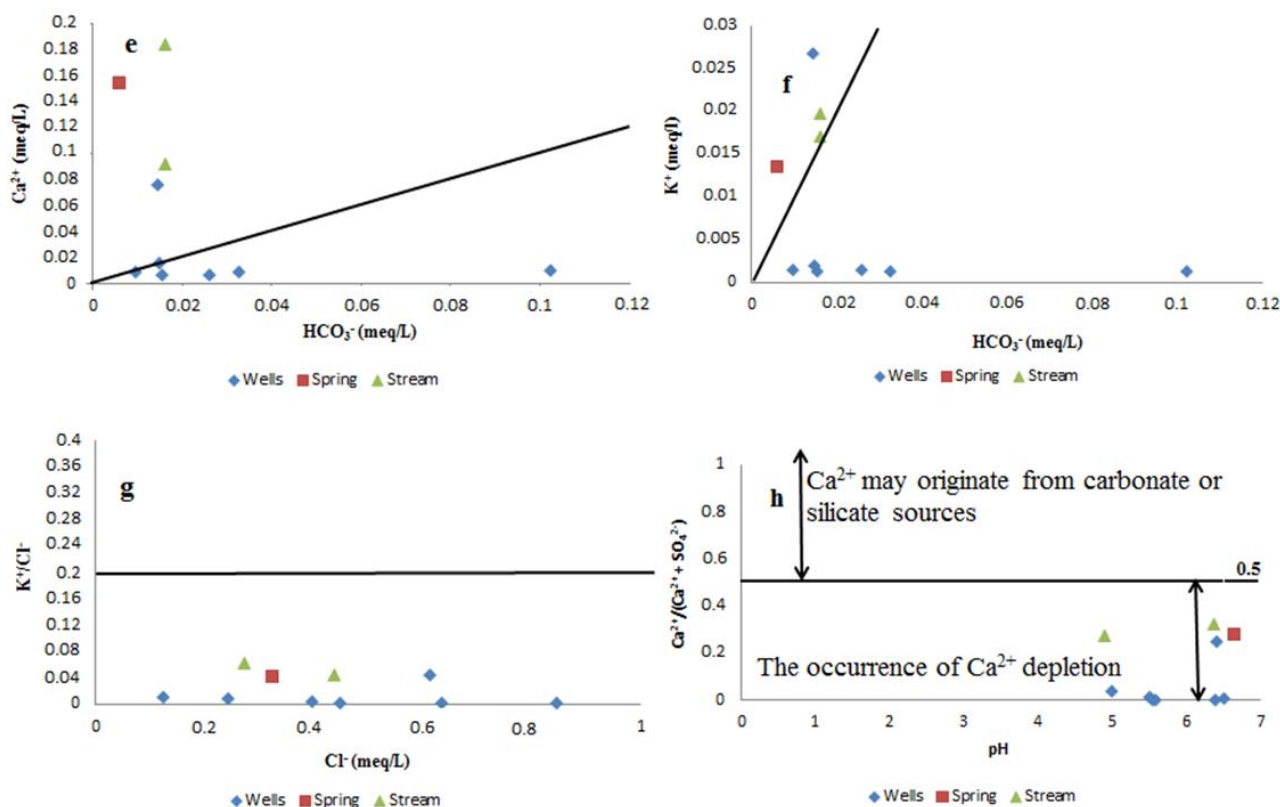


Figure 5. Relationships between major ion concentrations of water samples of study area to discriminate hydrochemical processes. (a) ($\text{Ca}^{2+} + \text{Mg}^{2+}$) vs. HCO_3^- , (b) ($\text{Ca}^{2+} + \text{Mg}^{2+}$) vs. $\text{HCO}_3^- + \text{SO}_4^{2-}$, (c) Mg^{2+} vs. Ca^{2+} , (d) Cl^- vs. Na^+ , (e) Ca^{2+} vs. HCO_3^- , (f) K^+ vs. HCO_3^- , (g) K^+/Cl^- vs. Cl^- , (h) $\text{Ca}^{2+}/(\text{Ca}^{2+} + \text{SO}_4^{2-})$ vs. pH.

3.5. Anthropogenic Controls on Water Quality

The objective of this part of the study is to ascertain the provenance of components that do not demonstrate a correlation with Total Dissolved Solids (TDS) and appear to be unrelated to geology. Figure 6 provides a visual representation of this through the plotting of Cl^- versus NO_3^- , Cl^- versus SO_4^{2-} , NO_3^- versus SO_4^{2-} , and NO_3^- versus K^+ . The figure elucidates the presence of strong correlations between Cl^- and NO_3^- and between Cl^- and SO_4^{2-} , signifying the presence of mixed or analogous anthropogenic inputs. The water type Ca-Mg-Cl- SO_4 observed in the piper diagram indicates a significant impact of anthropogenic activities. A robust correlation has been identified between chlorides and nitrates, suggesting a common origin for these components and implicating them in laundry and sanitation practices, such as the use of effluent from latrines. However, chloride and sulphate ions have been found to predominate in the laundry waters of domestic sources. Furthermore, Figure 6 demonstrates an association between K^+ and NO_3^- and SO_4^{2-} and NO_3^- . The increase in nitrate levels, excluding potassium, indicates that the observed growth is not attributable to pollution from fertilizers used in agriculture. As posited by [41, 105], the oxidation-reduction reactions of organic matter associated with septic-tank effluent, animal, or plant production are predom-

inantly accountable for the occurrence of nitrates in this area.

In order to also evaluate the impact of human activities on the water in Mbankomo, the percentage of pollution and agriculture were determined. The values of the pollution index (PI) vary between 94.80 and 99.74%, with an average of 98.86%. Areas with a PI < 40% are dominated by weathering reactions, while those with a PI > 40% are dominated by pollution. Subsequent to the initial observation, the overall pollution level in the area exhibiting PI > 40% was found to be 100% (Figure 7).

The percentage of agriculture exhibited significant variation, ranging from 66.47% to 94.55%, with an average of 82.08%. It is evident that regions exhibiting a percentage of agricultural activity in excess of 50% are subject to the repercussions of agricultural endeavors. Conversely, those demonstrating a percentage of agricultural activity that is less than 50% are influenced by the consequences of urban pollution and atmospheric inputs [57, 58]. However, the combination of pollution and agriculture enables the delineation of the composition of water into three classes, as defined by [58]: The classification system is comprised of three distinct classes: (1) weathering class, characterised by natural geogenic weathering processes with a PI < 40%; (2) effluent class, characterised by a PI > 40% and % agriculture < 50%; and (3) fertilization class, characterised by a PI > 40% and % agriculture > 50%. The classification system is the foundation for

the subsequent analysis, which indicates that all the water samples were dominated by agricultural pollution [57, 89]. The observations indicate that the study area is influenced by

agriculture, urban pollution, and the atmosphere, with implications for the suitable use of untreated water.

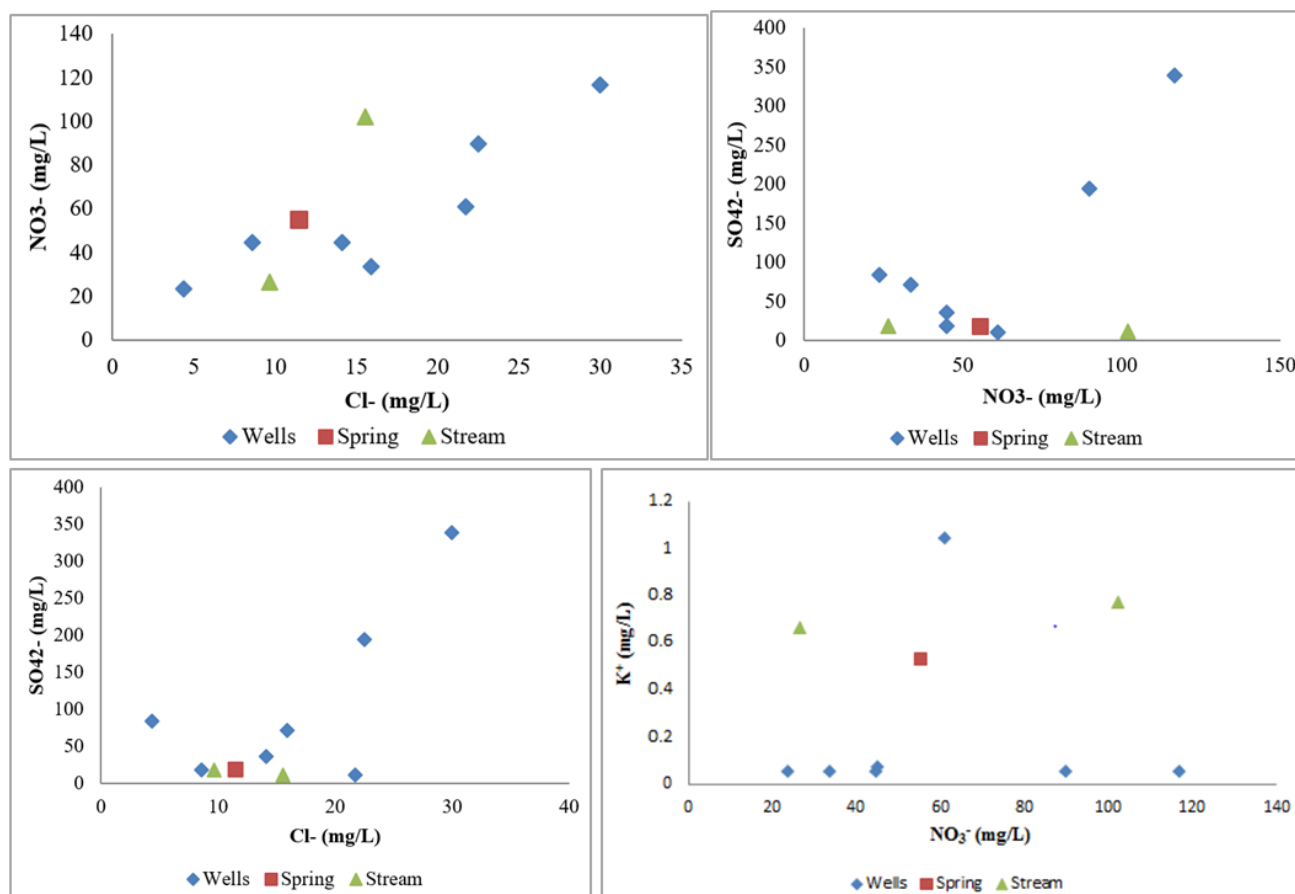


Figure 6. Relationship between NO_3^- vs Cl^- , SO_4^{2-} vs NO_3^- , Cl^- vs SO_4^{2-} and K^+ vs SO_4^{2-} .

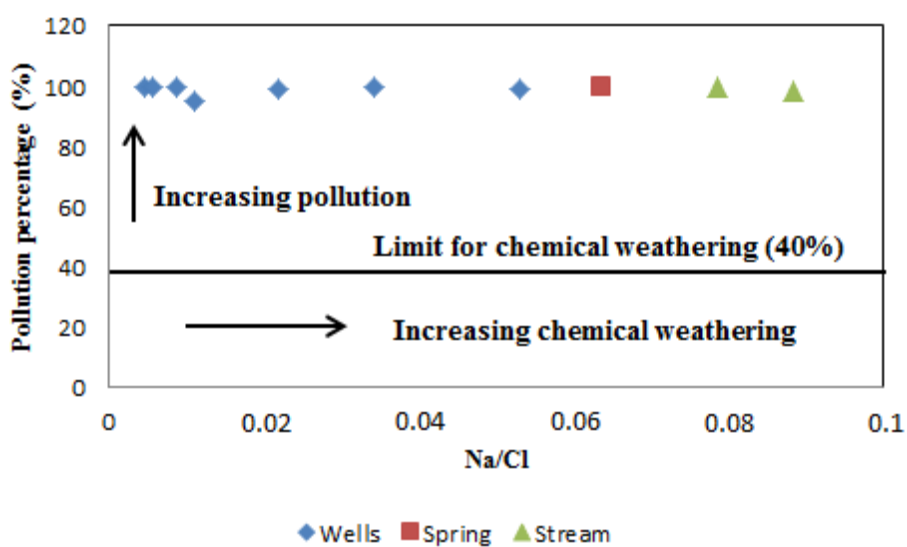


Figure 7. Variation in the percentage of pollution as a function of Na/Cl in water of study area.

3.6. Assessment of Water Suitability for Drinking and Irrigation Purpose

3.6.1. Water Quality Index (WQI)

The Water Quality Index (WQI) was calculated using the weighted arithmetic average method. The WQI calculation method is a rigorous approach that considers maximum permissible limits for any given regulation, whether it is national or international in scope. This method is adopted in accordance with the specific requirements of the study in question. This method is not without its limitations. For instance, it is not possible to evaluate all the risks present. Furthermore, weighting is required for every boundary as per its importance, which could be subjective. The results of the study indicated that the WQI in the designated area ranged from 17.18 to 47.52, with a mean value of 30.01 (table 4). The study found that 40% of samples were classified as excellent, 60% as good. Based on this result, the water of the study area can use for drinking, irrigation and industry.

Table 4. WQI values location wise with water type for all the sampling sites.

Samples	WQI	Water type	Possible use
MBW1	38.00	Good	Potable water. Irrigation and industry
MBW2	34.07	Good	Potable water. Irrigation and industry
MBW3	47.52	Good	Potable water. Irrigation and industry
MBW4	39.15	Good	Potable water. Irrigation and industry
MBW5	21.36	Excellent	Potable water. Irrigation and industry
MBW6	18.90	Excellent	Potable water. Irrigation and industry
MBW7	33.89	Good	Potable water. Irrigation and industry
MBSP	24.77	Excellent	Potable water. Irrigation and industry
MBS1	17.18	Excellent	Potable water. Irrigation and industry
MBS2	25.26	Good	Potable water. Irrigation and industry

3.6.2. Water Quality Characteristics for Irrigation Purposes

Sodium Adsorption Ratio (SAR), Sodium Percentage (Na%), Kelly's Ratio (KR), Residual Sodium Carbonate

(RSC), Magnesium Adsorption Ratio (MAR), Potential Salinity (PS) have all been used to assess the suitability of water for irrigation. The suitability of water for irrigation has been graded using these indicators.

The most widely utilized method for determining the suitability of irrigation water is the Sodium Adsorption Ratio (SAR) [106]. An increase in sodium content in soil has been shown to result in the displacement of calcium and magnesium ions by sodium. This process has been found to induce deflocculation of the soil, leading to a decrease in the rate of infiltration and permeability. Furthermore, this shift in ion composition has been observed to reduce the availability of vital nutrients and water. Consequently, this has been demonstrated to result in decreased crop yields [107, 108]. Furthermore, soils that are affected by sodicity issues frequently encounter difficulties with water infiltration. Additionally, these soils may exhibit problems with their soil structure, which can result in diminished load-bearing capacity [109, 110]. The process under investigation has been shown to induce the dispersion of clay particles, thereby causing them to separate from one another. Consequently, the soil structure is characterized by the predominance of exceedingly fine pores, a phenomenon that substantially impedes both water movement and permeability [111, 112]. The mean value of the SAR values was found to be 0.10, with a range of 0.06 to 0.20. As demonstrated in Table 5, it is evident that all samples exhibit optimal compatibility for irrigation purposes. The investigation revealed that all the water samples fell within the C0S1 and C1S1 categories, indicating low salinity and low sodium levels indicating their suitability for irrigation without posing any alkalinity risk to crops. This finding is consistent with the classification system outlined in Figure 8, which employs a salinity diagram to categorize water samples based on their chemical composition.

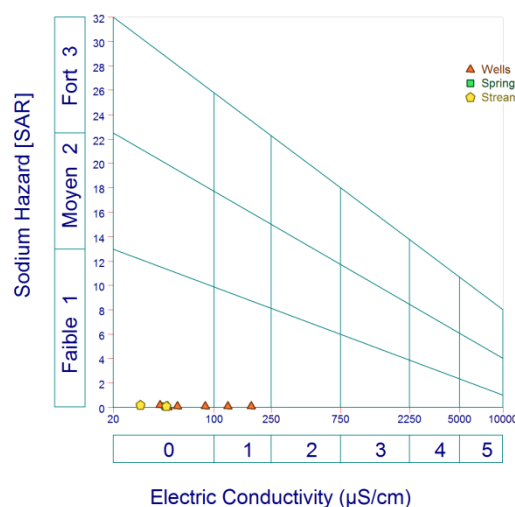


Figure 8. Suitability of water for irrigation from Riverside diagrams.

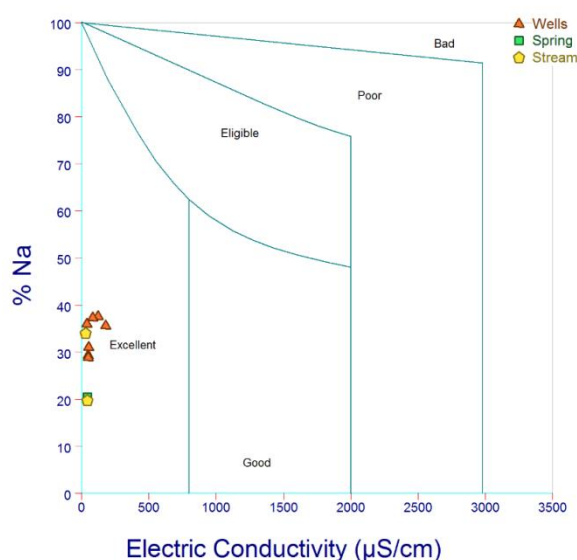


Figure 9. Suitability of water for irrigation from Wilcox diagrams.

One important factor in evaluating whether water is suitable for irrigation is its percent salt content. When used for irrigation, high salt content of the water may hinder plant growth and decrease soil permeability [113]. The Na^+ percentage ranged from 16.85 to 48.86% in with an average of 35.43%, (table 5). The quality of water intended for irrigation of crops exhibited a range of excellent quality base for this ratio. In accordance with the Wilcox classification [114], the water samples exhibited a range of excellent quality for irrigation purposes (Figure 9).

The SSP values of the water samples from the study area ranged from 19.76 to 37.57% with an average of 31.01%. Based on the SSP classification, all water samples had values

less than 60% and were therefore considered safe for irrigation (Table 5).

The RSC has been demonstrated to be a valuable tool for the assessment of irrigability through the CO_3^{2-} and HCO_3^- ratio [115]. A negative RSC value was observed in 60% of the samples collected, indicating that Na^+ is the predominant cation. An excess of Na^+ has been shown to compensate for Ca^{2+} and Mg^{2+} ions by precipitating them as CO_2 . Nevertheless, 40% of the samples exhibited a positive RSC value, suggesting elevated concentrations of HCO_3^- via Ca^{2+} and Mg^{2+} ions in the form of calcium bicarbonate and magnesium bicarbonate [116]. In addition, [117] classified water quality based on RSC values as follows: good ($\text{RSC} < 1.25$), moderately suitable ($1.25 < \text{RSC} < 2.5$), and unsuitable ($\text{RSC} > 2.5$). The calculated average RSC value in the study area was -0.05 meq/l, with a range of -0.20 to 0.08 meq/l. As demonstrated in Table 5, all of the water samples were classified as being of the good water quality.

The range of KI values was from 0.17 to 0.49, with an average value of 0.35. It is evident from the KI evaluation that all the waters are deemed suitable for irrigation practices ($\text{KI} < 1$) (Table 5).

The range of MAR values is from 12.66 to 46.49, with an average value of 36.10. It is evident that, in accordance with the water classification for MAR, the water can be regarded as being suitable for irrigation (< 50). An elevated magnesium concentration has been demonstrated to augment the alkalinity of the soil, thereby impeding its capacity for infiltration [118-120].

The PS values range from 0.43 to 4.38 with a mean value of 1.27. According to the classification proposed by [121], the water samples were found to belong to the excellent to good category in relation to irrigation (Table 5).

Table 5. Water suitability based on different water quality index.

Parameters	Range	Class	N ° of sample	Percentage of sample
Na%	<200	Maximum allowable limit	MBW1. MBW2. MBW3. MBW4. MBW5. MBW6. MBW7. MBSP. MBS1. MBS2	100.0%
	>200	Above allowable limit		
SAR (Sodium Adsorption Ratio)	<20	Excellent	MBW1. MBW2. MBW3. MBW4. MBW5. MBW6. MBW7. MBSP. MBS1. MBS2	100.0%
	20-40	Good		
	40-60	Permissible		
	60-80	Doubtful		
	>80	Unsuitable		
TDS (mg/l)	< 450	Excellent	MBW1. MBW2. MBW3. MBW4. MBW5. MBW6. MBW7. MBSP. MBS1. MBS2	100.0%

Parameters	Range	Class	N ° of sample	Percentage of sample
	450-2000	Moderate		
KR	< 1	Safe	MBW1. MBW2. MBW3. MBW4. MBW5. MBW6. MBW7. MBSP. MBS1. MBS2	100.0%
	> 1	Unsafe		
MAR (%)	< 50	Safe	MBW1. MBW2. MBW3. MBW4. MBW5. MBW6. MBW7. MBSP. MBS1. MBS2	100.0%
	> 50	Unsafe		
PS (meq/L)	< 5	Excellent to good	MBW1. MBW2. MBW3. MBW4. MBW5. MBW6. MBW7. MBSP. MBS1. MBS2	100.0%
	5-10	Good to injurious		
	> 10	Injurious to unsatisfactory		
RSC (meq/L)	< 1.25	Good	MBW1. MBW2. MBW3. MBW4. MBW5. MBW6. MBW7. MBSP. MBS1. MBS2	100.0%
	1.25-2.5	Doubtful		
	> 2.5	Unsuitable		
CAI-1	< 0	Class-I	MBW1. MBW2. MBW3. MBW4. MBW5. MBW6. MBW7. MBSP. MBS1. MBS2	100.0%
	> 0	Class-II		
CAI-2	< 0	Class-I	MBW1. MBW2. MBW3. MBW4. MBW5. MBW6. MBW7. MBSP. MBS1. MBS2	100.0%
	> 0	Class-II		

4. Conclusion

The commune of Mbankomo is situated in the Centre Region of Cameroon between 11°13' and 11°39' east longitude and 3°37' and 3°57' north latitude. Due to population growth, uncontrolled urbanization and the lack of an adequate water supply system, the area's water resources are under significant stress. The main objective of this work was to provide a comprehensive evaluation of water quality, highlighting the implications for sustainable water management practices. In light of the results obtained, water resources of the study area is acid (pH>7) for human consumption. The mineralization levels in surface water range from low to medium, while groundwater exhibits extremely weak mineralization. Piper diagram illustrates only one facies: Ca-Mg-Cl-SO₄ which exhibit anthropogenic effect on water. Water in the research area acquires mineralization through a variety of natural geochemical processes, such as weathering, dissolution, ion exchange processes, and human activity. The order of abundance of cations and anions concentrations is as follow Ca²⁺ > Na⁺ > K⁺ > Mg²⁺ > NH₄⁺ and SO₄²⁻ > NO₃⁻ > Cl⁻ > HCO₃⁻ > F⁻ > PO₄³⁻.

The combination of percentage of pollution index and

percentage of agriculture index indicates that the study area is influenced by agriculture, urban pollution, and the atmosphere, with implications for the suitable use of untreated water. The classification of the waters from the salinity diagram indicate low salinity and low sodium water. Henceforth, these water are suitable for irrigation for almost all types of crops with a possibility of limited sodium hazards. It is now urgent for decision-makers to implement protocols for the protection and treatment of water resources of the study area which are subject to agricultural pollution. As a perspective, it will be intended to increase the sample size to cover the entire study area and reinforce the results obtained here. Furthermore, an isotopic study will be carried out in order to better understand the origin of the mineralization of the water.

Abbreviations

TDS	Total Dissolved Solid
WQI	Water Quality Index
pH	Potential of Hydrogen
EC	Electrical Conductivity
EDTA	Ethylene Diamine Tetraacetic Acid
HPLC	High Performance Liquid Chromatography

SAR	Sodium Absorption Ratio
KR	Kelly Ratio
SSP	Soluble Sodium Percentage
RSC	Residual Sodium Carbonate
MAR	Magnesium Absorption Ratio
PS	Potential Salinity
WHO	World Health Organization
CAI	Chloro-alkaline Index

Conflicts of Interest

The authors declare no conflicts of interest.

References

- [1] Ofosu, S. A., Adjei, K. A., & Odai, S. N. Assessment of the quality of the Densu river using multicriterial analysis and water quality index. *Applied Water Science*. 2021, 11(12), 183. <https://doi.org/10.1007/s13201-021-01516-z>
- [2] Hosseini, M., Hassanzadeh, R. Groundwater quality assessment for domestic and agricultural purposes using GIS, hydrochemical facies and water quality indices: case study of Rafsanjan plain, Kerman province, Iran. *Applied Water Science*. 2023, 13(3), 84. <https://doi.org/10.1007/s13201-023-01891-9>
- [3] Jalali, M., Shademani, M., Paripour, M., Jalali, M. Assessment of water quality for mountainous high-elevated spring waters using self-organized maps. *Groundwater for Sustainable Development*. 2024, vol. 24. <https://doi.org/10.1016/j.gsd.2024.101082>
- [4] Varis, O. Resources: Curb vast water use in central Asia. *Nature* 514, 27-29. 2014. <https://doi.org/10.1038/514027a>
- [5] Cantillana, R., Molina, J. L., Iniesta-Arandia, I. Bringing water values into play in the Atacama desert water crisis, *Journal of Arid Environments*. 2024, Volume 225, 105256, ISSN 0140-1963, <https://doi.org/10.1016/j.jaridenv.2024.105256>
- [6] Zhang, Y., Chen, Z., Huang, G., Yang, M. Origins of groundwater nitrate in a typical alluvial-pluvial plain of North China plain: New insights from groundwater age-dating and isotopic fingerprinting. *Environmental Pollution*. 2023, 316, 120592. <https://doi.org/10.1016/j.envpol.2022.120592>
- [7] Chen, K., Liu, Q., Yang, T., Ju, Q., Zhu, M. Risk assessment of nitrate groundwater contamination using GIS-based machine learning methods: A case study in the northern Anhui plain, China. *Journal of Contaminant Hydrology*. 2024, 261, 104300. <https://doi.org/10.1016/j.jconhyd.2024.104300>
- [8] Rashid, I., Naqvi, S. N. H., Mohsin, H., Fatima, K., Afzal, M., Al-Misned, F., ... Niazi, N. K. The evaluation of bacterial-augmented floating treatment wetlands for concomitant removal of phenol and chromium from contaminated water. *International journal of phytoremediation*. 2024. 26(2), 287-293. <https://doi.org/10.1080/15226514.2023.2240428>
- [9] Chen, K., Liu, Q., Peng, W., Liu, X. Source apportionment and natural background levels of major ions in shallow groundwater using multivariate statistical method: a case study in Huaibei Plain, China. *J Environ Manag*. 2022, 301: 113806. <https://doi.org/10.1016/j.jenvman.2021.113806>
- [10] Gao, J., Deng, G., Jiang, H., Wen, Y., Zhu, S., He, C., Cao, Y. Water quality pollution assessment and source apportionment of lake wetlands: A case study of Xianghai Lake in the Northeast China Plain. *Journal of Environmental Management*. 2023, 344, 118398. <https://doi.org/10.1016/j.jenvman.2023.118398>
- [11] Subba Rao, G., Harsha, G. S., Jeelani, S. H., Rizvi, S. S., Roy, S. K., Manjaly, M. S. Groundwater Quality Assessment for Drinking and Irrigational Purposes Using Water Quality Index (WQI) of Dubbak (M), Siddipet District, Telangana, India. In *International Conference on Advances in Environmental Sustainability, Energy and Earth Science*. 2024, (pp. 271-297). AESEE 2024. Springer, Cham. https://doi.org/10.1007/978-3-031-73820-3_19
- [12] Chaudhary, R., Gaur, N., Yadav, M. Hydrogeochemical analysis of groundwater quality during the pre-monsoon season of Manipur, India. *Water Science*. 2024, 38(1), 274-292. <https://doi.org/10.1080/23570008.2024.2341369>
- [13] Giridharan, L., Venugopal, T., Jayaprakash, M. Evaluation of the seasonal variation on the geochemical parameters and quality assessment of the groundwater in the proximity of River Cooum, Chennai, India. *Environmental monitoring and assessment*. 2008, 143, 161-178. <https://doi.org/10.1007/s10661-007-9965-y>
- [14] Aly, A. A. Hydrochemical characteristics of Egypt western desert oases groundwater. *Arabian Journal of Geosciences*. 2015, 8(9), 7551-7564.
- [15] Aghazadeh, N., Chitsazan, M., & Golestan, Y. Hydrochemistry and quality assessment of groundwater in the Ardabil area, Iran. *Applied Water Science*. 2017, 7, 3599-3616. <https://doi.org/10.1007/s13201-016-0498-9>
- [16] Jahanshahi, R., Mahmoodinejad, N., & Mali, S. Hydrogeochemistry and groundwater origin in the Sarduiyeh area, Iran. *Geopersia*, 2025. <https://doi.org/10.22059/geope.2025.390781.648810>
- [17] Nzenti, J. P., Barbey, P., Macaudier, E. J., Soba, D. Origin and evolution of the late Precambrian high grade Yaoundé gneiss (Cameroon). *Precambrian Research*. 1988, 38, pp 91 - 109. [https://doi.org/10.1016/0301-9268\(88\)90086-1](https://doi.org/10.1016/0301-9268(88)90086-1)
- [18] Nzenti, J. P. Neoproterozoic alkaline meta-igneous rocks from the Pan-African North Equatorial Fold Belt (Yaoundé, Cameroon): biotites and magnetite rich pyroxenites. *Journal of African Earth Sciences*. 1998. 26(1), 37-47. [https://doi.org/10.1016/S0899-5362\(97\)00135-8](https://doi.org/10.1016/S0899-5362(97)00135-8)
- [19] Toteu, S. F., Penaye, J., Djomani, P. Y. Evolution géodynamique de la ceinture panafricaine en Afrique centrale avec une référence particulière au Cameroun. *Revue canadienne des sciences de la Terre*. 2004, 41(1): 73-85. <https://doi.org/10.1139/E03-079>

- [20] Metang, V., Nomo Negue, E., Ganno, S., Takodjou Wambo, J. D., Ewolo Teme, A. M., Teda Soh, A. C., Fossi, D. H., Nkanga Mbakam, M. D., Tchameni, R., Nzenti, J. P. Anatexis of metadiorite from the Yaounde area, central african orogenic belt in Cameroon: implications on the genesis of in-source granodiorite leucosomes. *Arabian Journal of Geosciences*. 2022, 15(4), 359. <https://doi.org/10.1007/s12517-022-09642-x>
- [21] Mvondo, H. Analyses structurale et pétro géochimique des roches de la région de Yaoundé Nord: Arguments contribuant à la connaissance de l'évolution géotechnique de la chaîne panafricaine au Cameroun. Thèse Doct. Univ. YdéI. 2003, 173 p.
- [22] Djeuda Tchapinga, H. B., Tanawa, E., Ngnigam, E. L'eau au Cameroun: Approvisionnement en Eau Potable (Tome 1). Presses Universitaires Yaoundé 2001, 359 p.
- [23] Djeuda Tchapinga, H. B. Géologie et hydrogéologie d'un secteur de la zone mobile d'Afrique centrale: région de poli, nord - Cameroun. Thèse doct. Univ. sci. tech. et mál. de Grenoble 1, France. 1987, 333 p.
- [24] Wyns, R. Ressources en eau de la Margeride ouest - PRD 324 - Modélisation de la géomorphie (altitude, épaisseur) des arènes granitiques du bassin-versant lozérien de la Truyère (Lozère, Massif Central). Rapport BRGM R. 1998, 40191, 18 p.
- [25] Taylor, R., Howard, K. A tectono-geomorphic model of the hydrogeology of deeply weathered crystalline rock: Evidence of Uganda. *Hydrogeologie journal*. 2000, (8): 279-294. <https://doi.org/10.1007/s100400000069>
- [26] Maréchal, J. C., Wyns, R., Lachassagne, P., Subrahmanyam, K., Touchard, F. Vertical anisotropy of hydraulic conductivity in fissured layer of hard-rock aquifers due to the geological structure of weathering profiles. *Comptes Rendus. Géoscience*. 2003, 335(5), 451-460. [https://dx.doi.org/10.1016/s1631-0713\(03\)00082-8](https://dx.doi.org/10.1016/s1631-0713(03)00082-8)
- [27] Lachassagne, P., Wyns, R. Aquifères de socle: nouveaux concepts. Application à la prospection et la gestion de la ressource en eau. *Géosciences*. 2005, (2), 32-37.
- [28] Ryan, A., Yeow, A., Swain, L. G., Webber, T. N. Water sampling procedures, safety and quality assurance. Environment Canada, BC Ministry of Environment. 2005.
- [29] Lienou, G. Impacts de la variabilité climatiques sur les ressources en eaux et les transports de matières en suspension de quelques bassins représentatifs au Cameroun. Thèse doctorat/Ph. D, Université de Yaoundé I. 2007, 405 p.
- [30] Kpoumié A. Hydroclimatologie et transports solides dans un écosystème tropical anthropisé d'Afrique centrale dans un contexte déficitaire: cas du bassin versant de la Sanaga au Cameroun. Thèse doctorat/Ph. D, Université de Yaoundé I. 2015, 241 p.
- [31] Ndam Ngoupayou, J. R., Dzana, J. G., Kpoumie, A., Ghogomu, R. T., Fouepe Takounjou, A., Braun, J. J., Ekodeck, G. E. Present-day sediment dynamics of the Sanaga catchment (Cameroon): from the total suspended sediment (TSS) to erosion balance. *Hydrological Sciences Journal*. 2016, 61(6), 1080-1093. <https://doi.org/10.1080/02626667.2014.968572>
- [32] Rakotondrabe, F., Ngoupayou, J. R. N., Mfonka, Z., Rasolomanana, E. H., Abolo, A. J. N., & Ako, A. A. (2017). Water quality assessment in the Bataré-Oya gold mining area (East-Cameroon): multivariate statistical analysis approach. *Science of the total environment*, 610, 831-844. <https://doi.org/10.1016/j.scitotenv.2017.08.080>
- [33] Apha, A., 2012. Standard methods for the examination of water and wastewater, 22nd edition edited by E. W. Rice, R. B. Baird, A. D. Eaton and L. S. Clesceri. American Public Health Association (APHA), American Water Works Association (AWWA) and Water Environment Federation (WEF), Washington, D. C., USA.
- [34] Bon, A. F., Aoudou, D. S., Banakeng, A. L., Narke, C., Chouto, S., Ndam Mbouombouo, A., 2020. Contribution of a geostatistical model of electrical conductivity in the assessment of the water pollution index of the Quaternary aquifer of the Lake Chad basin (KousseriCameroon) *Arab. J. Geosci.* 13(4), 170. <https://doi.org/10.1007/s12517-020-5142-1>
- [35] Ngo Billong, P. T., Feumba, R., Ndjigui, P. D., 2023. Hydro-geochemical appraisal of groundwater quality in Ngoua watershed (Douala-Cameroon): Implication for domestic purposes. *Scientific African* 22(2023) e01910. <https://doi.org/10.1016/j.sciaf.2023.e01910>
- [36] Mfonka, Z., Morbe Mbadngonel, C., Nsangou, D., Kpoumié A., Kouassy Kaléjé P. S., Zammouri, M., Jules Ngoupayou, J. R., 2024. Groundwater quality assessment for drinking and agricultural purposes under arid climate in N'Djamena, Chad (Central Africa). *Inter. J. of Energy and Water Resources* <https://doi.org/10.1007/s42108-024-00297-w>
- [37] Gevorgyan, G., Khachatryan, G., Varagyan, A., Varagyan, V., Vaseashta, A. Hydrochemical Characterization, Source Identification, and Irrigation Water Quality Assessment in the Voghji River Catchment Area, Southern Armenia. *Water*. 2025, 17, 854. <https://doi.org/10.3390/w17060854>
- [38] Schoeller, H. Sur la concentration des sels dissous dans les eaux souterraines. The concentration of dissolved salts in groundwater. Rabat, Morocco In French. Comité Etudes eaux souterraines, Rabat Maroc. 1934, pp 46-54.
- [39] Laxman, K. D., Dhakate, R., Guguloth, S., Srinivas, B. Hydrochemical appraisal of groundwater quality for drinking and agricultural utility in a granitic terrain of Maheshwaram area of Ranga Reddy district (India). *Hydroresearch*. 2021, 4, 11-21. <https://doi.org/10.1016/j.hydres.2021.02.002>
- [40] Kumar, P., Vishwakarma, C. A., Singh, P., Rena, H. A. V., Mate, C. C., Mukherjee, S. Hydrogeochemical characterization and water quality evaluation for drinking and irrigation purposes of coastal aquifers of Middle Andaman. *Discover Applied Sciences*. 2024, 6(5), 228. <https://doi.org/10.1007/s42452-024-05889-z>
- [41] Bello, M., Ketchemen, T. B., Nlend, B., Huneau, F., Fouepe, A., Fantong, W. Y., Ngo Boum-Nkot, S., Garel, E., Celle-Jeanton, H. Shallow groundwater quality evolution after 20 years of exploitation in the southern Lake Chad: hydrochemistry and stable isotopes survey in the far north of Cameroon. *Environ. Earth Sci.* 2019, 78, 1-19 <https://doi.org/10.1007/s12665-019-8494-7>

- [42] Haman, D. J. B., Fantong, Y. W., Ewodo Mboudou, G., Om-bolo, A., Nenkam Jokam, T. L. L., Chounna, G. Y., Messi, G. Hydrogeochemistry and stable isotopes of groundwater in the Sudano-Sahelian zone: A case of the Mayo Bocki watershed in North Cameroon. *HydroResearch*. 2023, 36-51. <https://doi.org/10.1016/j.hydres.2023.01.002>
- [43] Venkatesan, S., Arumugam, S., Bagyaraj, M., Preethi, T., & Parthasarathy, P. Spatial assessment of Groundwater Quantity and Quality: A case study in parts of Chidambaram Taluk, Cuddalore District, Tamil Nadu, India. *Sustainable Water Resource Management*. 2021, 7, 103. <https://doi.org/10.1007/s40899-021-00585-x>
- [44] Al Haj, R., Merheb, M., Halwani, J., Ouddane, B. Hydrogeo-chemical characteristics of groundwater in the Mediterranean region: A meta-analysis. *Physics and Chemistry of the Earth*. 2022, 129, 103351. <https://doi.org/10.1016/j.pce.2022.103351>
- [45] Rahman, M. S., Selim Reza, A. H. M., Ahsan, M. A., Bakar Siddique, M. A. Arsenic in groundwater from Southwest Bangladesh: Sources, water quality, and potential health concern. *HydroResearch*. 2023, 6, 1-15. <https://doi.org/10.1016/j.hydres.2022.12.001>
- [46] Bouteraa, O., Mebarki, A., Bouaicha, F., Nouaceur, Z., & Laignel, B. Groundwater quality assessment using multivariate analysis, geostatistical modeling, and water quality index (WQI): a case of study in the Boumerzoug-El Khroub valley of Northeast Algeria. *Acta Geochimica*. 2019. 38, 796-814. <https://doi.org/10.1007/s11631-019-00329-x>
- [47] Jena, P. K., Rahaman, S. M., Das Mohapatra, P. K., Barik, D. P., & Patra, D. S.. Surface water quality assessment by Random Forest. *Water Practice & Technology*. 2023, 18(1), 201-214. <https://doi.org/10.2166/wpt.2022.156>
- [48] Talhaoui A, El Hmaidi A, Jaddi H, Habiba Ousmana H, Manssouri I. Calculation of the Water Quality Index (WQI) for the Evaluation of the Physico-Chemical Quality of Surface Waters of the Moulouya Wadi (NE, Morocco). *European Scientific Journal* January 2020 edition Vol.16, No.2 ISSN: 1857 - 7881 (Print) e - ISSN 1857- 7431. <https://doi.org/10.19044/esj.2020.v16n2p64>
- [49] Kadam A, Wagh V, Jacobs J, Patil S, Pawar N, Umrikar B, Sankhua R., Kumar S. Integrated approach for the evaluation of groundwater quality through hydro geochemistry and human health risk from Shivganga river basin, Pune, Maharashtra, India. *Environ. Sci. Pollut. Res.*, 2021, 1 -23. <https://doi.org/10.1007/s11356-021-15554-2>
- [50] Ngo Boum-Nkot S, Nlend B, Komba D, Nkoue Ndong GR, Bello M, Fongoh EJ, Ntamak-Nida MJ, Etame J. Hydro-chemistry and assessment of heavy metals groundwater contamination in an industrialized city of sub-Saharan Africa (Douala, Cameroon). *Implication on human health HydroResearch* 6(2023) 52-64. <https://doi.org/10.1016/j.hydres.2023.01.003>
- [51] Pimparkar AM, Patil SN, Patil BD, Kadam AK. Comparative assessment of wetland water quality from rural and urban area of Aurangabad District, Maharashtra, India using water quality index *HydroResearch* 6(2023) 269-278. <https://doi.org/10.1016/j.hydres.2023.10.001>
- [52] Goher, M. E., Hassan, A. M., Abdel-Moniem, I. A., Fahmy, A. H., & El-Sayed, S. M. Evaluation of surface water quality and heavy metal indices of Ismailia Canal, Nile River, Egypt. *Egyptian Journal of Aquatic Research*. 2014, 40(3), 225-233. <https://doi.org/10.1016/j.ejar.2014.09.001>
- [53] WHO. Directives de qualité pour l'eau de boisson: 4e éd. Intégrant le premier additif. 2017, 539 p.
- [54] Balamurugan P, Kumar PS, Shankar K, Dataset on the suitability of groundwater for drinking and irrigation purposes in the Sarabanga River region, Tamil Nadu, India. *Data Br*. 2020, 29, 105255. <https://doi.org/10.1016/j.dib.2020.105255>
- [55] Kawo NS, Karuppannan S. Groundwater quality assessment using water quality index and GIS technique in Modjo River basin, Central Ethiopia. *J. Afr. Earth Sci.*, 2018, 147, 300- 311. <https://doi.org/10.1016/j.jafrearsci.2018.06.034>
- [56] Gao Z, Han C, Xu Y, Zhao Z, Luo Z, Liu J.. Assessment of the water quality of groundwater in Bohai rim and the controlling factors a case study of northern Shandong peninsula, North China. *Environ. Pollut.* 2021, 85, 117482. <https://doi.org/10.1016/j.envpol.2021.117482>
- [57] Pacheco FAL, Van der Weijden CH. Contributions of water-rock interactions to the composition of groundwaters in areas with a sizeable anthropogenic input: a case study of the water of the Fundao area, central Portugal. *Water Resour Res*, 1996, 32(12): 3553-3570. <https://doi.org/10.1029/96WR01683>
- [58] Pacheco FAL. Application of correspondence analysis in the assessment of groundwater chemistry. *Math Geol.*, 1998, 30(2): 129-161. <https://doi.org/10.1023/A:1021718929576>
- [59] Todd, D. K. In: Jon, N. Y. (Ed.), *Groundwater Hydrology*. Wiley Sons Inc. 1980, 535 p.
- [60] Kelley, W. P. (1963). Use of saline irrigation water. *Soil science*, 95(6), 385-391.
- [61] Ghalib, H. B. Groundwater chemistry evaluation for drinking and irrigation utilities in east Wasit province, Central Iraq. *Applied Water Science*. 2017, 7, 3447-3467. <https://doi.org/10.1007/s13201-017-0575-8>
- [62] Eaton, F. M. Significance of carbonates in irrigation waters. *Soil science*. 1950, 69(2), 123-134.
- [63] Raghunath, H. M. *Ground water: hydrogeology, ground water survey and pumping tests, rural water supply and irrigation systems*. New Age International. 1987, 549 p.
- [64] Szabolcs, I.; Darab, C. The Influences of Irrigation Water of High Sodium Carbonate Contents on Soils. In *Proceedings of the 8th International Congress Soil Science Sodic Soils*, Bucharest, Romania, 31 August-9 September 1964; pp. 802-812.
- [65] WHO. *Guidelines for Drinking-Water Quality. Recommendations*. 4th edition. World Health Organization, Geneva. 2011.

- [66] Zebaze Togouet, S. H., Boutin, C., Njiné T., Kemka, N., Nola, M., Menbohan, S. F. First data on the groundwater quality and aquatic fauna of some wells and springs from Yaounde (Cameroon). *European journal of water quality*. 2009, 40(1), 51-74. <https://doi.org/10.1051/water/2009005>
- [67] Zɔ́az éTogouet, S. H., Tuekam Kayo, R. P., Boutin, C., Nola, M., & Foto Menbohan, S. Impact de la pression anthropique sur l'eau et la faune aquatique des puits et sources de la région de Yaoundé (Cameroun, Afrique Centrale). *Bulletin de la société d'Histoire Naturelle de Toulouse*. 2011, 147, 27-41.
- [68] Wirmvem, M. J., Ohba, T., Fantong, W. Y., Ayonghe, S. N., Suila, J. Y., Asaah, A. N. E.,... Hell, J. V. Hydrochemistry of shallow groundwater and surface water in the Ndop plain, North West Cameroon. *African Journal of Environmental Science and Technology*. 2013, 7(6), 518-530. <https://doi.org/10.5897/AJEST2013.1456>
- [69] Tuekam, R. P., Nyamsi Tchactcho, N. L., Noah Ewoti, V., Chinche, SB., Nzi deu, J. G., Poutougnigni, O. F., Zɔ́az éS. H. Physicochemical characterization dynamics abundance bacteriological and aquatic fauna of groundwater in the city of Mbalmayo (Cameroon). *Journal of biodiversity and environment science*. 2021, 13(2), 1 -15.
- [70] Tamonkem, R. A., Tchouta, K. D., Mvondo V. Y. E., Iwoudam M. E., Ngounou Ngatcha B. Contribution of Piezometry and Hydro-Geochemistry to a Better Understanding of the Adamawa-Yadé Hard Rock Aquifer System in Ngaoundéré American Journal of Water Resources. 2024. 12(2), 39-52. <https://doi.org/10.12691/ajwr-12-2-2>
- [71] Takang, A. V., Wotany, E. R., Agyinyi C. Evaluation of surface water quality for domestic and agro-industrial applications along the tropical rainforest gradient, central Cameroon. 2025, 19(3), 89-105, <https://doi.org/10.5897/AJEST2025.3322>
- [72] Yongue-Fouateu, R. Contribution à l'étude pétrographique de l'altération et des faciès de cuirassement ferrugineux des gneiss migmatitiques de la région de Yaoundé Univ. Yaoundé 1986. 214 p.
- [73] Ndam Ngoupayou, J. R. Bilans hydrochimiques sous forêt tropicale humide en Afrique: exemple du bassin expérimental de Nsimi-Zoé dé au réseau hydrographique du Nyong et de la Sanaga (Sud Cameroun). Thèse Univ. de Paris IV. 1997, 214 p.
- [74] Mfonka, Z., Kpoumie, A. C., Ngouh, A. N., Ndam Ngoupayou, J. R. Groundwater quality assessment under the arid climate zone in the Central Africa: case study of the South-west of N'Djamena. *Journal of Water Resource and Protection*. 2020, 13(2), 112-138. <https://doi.org/10.4236/jwarp.2025.175016>
- [75] Bon, A. F., Ngoss, T. A. M. N., Mboudou, G. E., Banakeng, L. A., Ngoupayou, J. R. N., & Ekodeck, G. E. Groundwater flow patterns, hydrogeochemistry and metals background levels of shallow hard rock aquifer in a humid tropical urban area in sub-Saharan Africa-A case study from Olézoa watershed (Yaoundé-Cameroon). *Journal of Hydrology: Regional Studies*. 2021, 37, 100904. <https://doi.org/10.1016/j.ejrh.2021.100904>
- [76] Dash, S., Kalamdhad, A. S. Hydrochemical dynamics of water quality for irrigation use and introducing a new water quality index incorporating multivariate statistics. *Environmental Earth Sciences*. 2021, 80(3), 73. <https://doi.org/10.1007/s12665-020-09360-1>
- [77] Freeze RA, Cherry JA, Groundwater. Englewood, New Jersey: Prentice-Hall Inc., 1979.
- [78] Takounjou, A. F., Ndam Ngoupayou, J. R., Riotte, J., Takem, G. E., Mafany, G., Marechal, J. C., Ekodeck, G. E. Estimation of groundwater recharge of shallow aquifer on humid environment in Yaounde, Cameroon using hybrid water-fluctuation and hydrochemistry methods. *Environ. Earth Sci*. 2011, 64(1): 107-118. <https://doi.org/10.1007/s12665-010-0822-x>
- [79] Edmunds, W. M., Smedley, P. L. Groundwater geochemistry and health: an overview. Geological Society, London, Special Publications. 1996, 113(1), 91-105. <https://doi.org/10.1144/GSL.SP.1996.113.01.08>
- [80] Piper, A. M. A graphic procedure in the geochemical interpretation of water - analyses. *Eos, Transactions American Geophysical Union*. 1944, 25(6), 914-928. <https://doi.org/10.1029/TR025i006p00914>
- [81] Gibbs, R. J. Mechanisms controlling world water chemistry. *Science*. 1970, 170(3962), 1088-1090. <https://doi.org/10.1126/science.170.3962.1088>
- [82] Marandi, A., Shand, P. Groundwater chemistry and the Gibbs Diagram. *Applied Geochemistry*. 2018, 97, 209-212. <https://doi.org/10.1016/j.apgeochem.2018.07.009>
- [83] Bon, A. F., Abderamane, H., Ewodo Mboudou, G., Aoudou Doua, S., Banakeng, L. A., Bontsong Boyomo, S. B., & Wangbara Damo, B.. Parametrization of groundwater quality of the Quaternary aquifer in N'Djamena (Chad), Lake Chad Basin: Application of numerical and multivariate analyses. *Environmental Science and Pollution Research*. 2020b, 28, 12300-12320. <https://doi.org/10.1007/s11356-020-10622-5>
- [84] Menti, A. N., Wotany, E. R., Christopher, A., Wirmvem, M. J., & Ngai, N. J. Hydrogeochemical characterization of ground and surface water in the eastern part of the Adamawa-Yade domain, Bertoua-Cameroon. *Discover Water*. 2023. 3(1), 10. <https://doi.org/10.1007/s43832-023-00034-0>
- [85] Cendon, D. I., Larsen, J. R., Jones, B. G., Nanson, G. C., Rickleman, D., Hankin, S. I., Pueyo, J. J., Maroulis, J. Freshwater recharge into a shallow saline groundwater system, Cooper Creek floodplain, Queensland, Australia. *J. Hydrol*. 2010, 392(2-4): 150-163. <https://doi.org/10.1016/j.jhydrol.2010.08.003>
- [86] Tay, C. K. Hydrochemistry of groundwater in the Savelugu-Nanton District, Northern Ghana. *Environ. Earth Sci*. 2012, 67: 2077-2087. <https://doi.org/10.1007/s12665-012-1647-6>
- [87] Demlie M, Wohnlich S, Wisotzky F, Gizaw B. Groundwater recharge, flow and hydrogeochemical evolution in a complex volcanic aquifer system, central Ethiopia. *Hydrogeol. J*. 2007, 15: 1169-1181. <https://doi.org/10.1007/s10040-007-0163-3>

- [88] Fantong WY, Satake H, Ayonghe SN, Aka FT, Asai K. Hydrogeochemical controls and usability of groundwater in semi-arid Mayo Tsanaga River Basin, Far-North Cameroon. *Environ. Geol.* 2009, 58(6): 1281-1293. <https://doi.org/10.1007/s00254-008-1629-x>
- [89] Prasanna, M. V., Nagarajan, R., Chidambaram, S., Anand Kumar, A., & Thivya, C. Evaluation of hydrogeochemical characteristics and the impact of weathering in seepage water collected within the sedimentary formation. *Acta Geochimica.* 2017, 36, 44-51. <https://doi.org/10.1007/s11631-016-0125-3>
- [90] Yang, Q., Li, Z., Ma, H., Wang, L., Martín, J. D. Identification of the hydrogeochemical processes and assessment of groundwater quality using classic integrated geochemical methods in the Southeastern part of Ordos basin, China. *Environmental Pollution.* 2016, 218, 879-888. <https://doi.org/10.1016/j.envpol.2016.08.017>
- [91] Gopinath, S., Srinivasamoorthy, K., Saravanan, K., Prakash, R. Tracing groundwater salinization using geochemical and isotopic signature in Southeastern coastal Tamilnadu, India. *Chemosphere.* 2019, 236, 124305. <https://doi.org/10.1016/j.chemosphere.2019.07.036>
- [92] Liu, J., Peng, Y., Li, C., Gao, Z., & Chen, S. An investigation into the hydrochemistry, quality and risk to human health of groundwater in the central region of Shandong Province, North China. *Journal of cleaner production.* 2021, 282, 125416. <https://doi.org/10.1016/j.jclepro.2020.125416>
- [93] Gopal Krishan, Kumar M., Rao, M. S., Garg, R., Yadav, B. K., Kansal, M. L., Singh, S., Bradley, A., Muste, M., Sharma L. M. Integrated approach for the investigation of groundwater quality through hydrochemistry and water quality index (WQI). *Urban Climate* 47. 2023, 101383, <https://doi.org/10.1016/j.uclim.2022.101383>
- [94] Okiongbo, K. S., Akpofure, E. Identification of hydrogeochemical processes in groundwater using major ion chemistry: a case study of Yenagoa and environs, southern Nigeria. *Global Journal of Geological Sciences.* 2014, 12, 39-52. <https://doi.org/10.4314/gjgs.v12i1.5>
- [95] Gao, Z., Liu, J., Feng, J., Wang, M., Wu, G. Hydrogeochemical characteristics and the suitability of groundwater in the alluvial-diluvial plain of southwest Shandong Province, China. *Water*, 2019, 11(8), 1577. <https://doi.org/10.3390/w11081577>
- [96] Sahu, S., Gogoi, U., & Nayak, N. C. Groundwater solute chemistry, hydrogeochemical processes and fluoride contamination in phreatic aquifer of Odisha, India. *Geoscience Frontiers.* 2021, 12(3), 101093. <https://doi.org/10.1016/j.gsf.2020.10.001>
- [97] Abdelshafy, M., Saber, M., Abdelhaleem, A., Abdelrazek, S. M., & Seleem, E. M. Hydrogeochemical processes and evaluation of groundwater aquifer at Sohag city, Egypt. *Scientific African.* 2019, 6, e00196. <https://doi.org/10.1016/j.sciaf.2019.e00196>
- [98] Sheikhy Narany, T., Ramli, M. F., Aris, A. Z., Sulaiman, W. N. A., Juahir, H., & Fakharian, K. Identification of the Hydrogeochemical Processes in Groundwater Using Classic Integrated Geochemical Methods and Geostatistical Techniques, in Amol Babol Plain, Iran. *The Scientific World Journal.* 2014(1), 419058. <https://doi.org/10.1155/2014/419058>
- [99] Kanagaraj, G., Elango, L., Sridhar, S. G. D., & Gowrisankar, G. Hydrogeochemical processes and influence of seawater intrusion in coastal aquifers south of Chennai, Tamil Nadu, India. *Environmental Science and Pollution Research.* 2018, 25, 8989-9011. <https://doi.org/10.1007/s11356-017-0910-5>
- [100] Li, P., Wu, J., Qian, H. Hydrogeochemistry and Quality Assessment of Shallow Groundwater in the Southern Part of the Yellow River Alluvial Plain (Zhongwei Section), Northwest China. *Earth Sci. Res. J.* 2014, 18, 27-38. <https://doi.org/10.15446/esrj.v18n1.34048>
- [101] Sajil Kumar, P. J., & James, E. J. Identification of hydrogeochemical processes in the Coimbatore district, Tamil Nadu, India. *Hydrological Sciences Journal.* 2016, 61(4), 719-731. <https://doi.org/10.1080/02626667.2015.1022551>
- [102] Liu, F., Wang, S., Yeh, T. C. J., Zhen, P., Wang, L., & Shi, L. Using multivariate statistical techniques and geochemical modelling to identify factors controlling the evolution of groundwater chemistry in a typical transitional area between Taihang Mountains and North China Plain. *Hydrological Processes.* 2020, 34(8), 1888-1905. <https://doi.org/10.1002/hyp.13701>
- [103] Li, P., Wu, J., Qian, H. et al. Hydrogeochemical Characterization of Groundwater in and Around a Wastewater Irrigated Forest in the Southeastern Edge of the Tengger Desert, Northwest China. *Expo Health.* 2016, 8, 331-348. <https://doi.org/10.1007/s12403-016-0193-y>
- [104] Juen, L. L., Aris, A. Z., Shan, N. T., Yusoff, F. M., Hashim, Z. Geochemical modeling of element species in selected tropical estuaries and coastal water of the Strait of Malacca. *Procedia Environmental Sciences.* 2015, 30, 109-114. <https://doi.org/10.1016/j.proenv.2015.10.019>
- [105] Huneau, F., Dakoure, D., Celle-Jeanton, H., Vitvar, T., Ito, M., Traore, S., Le Coustumer, P. Flow pattern and residence time of groundwater within the south-eastern Taoudeni sedimentary basin (Burkina Faso, Mali). *Journal of Hydrology.* 2011, 409(1-2), 423-439. <https://doi.org/10.1016/j.jhydrol.2011.08.043>
- [106] Othman, F., Farrag, A., Seleem, E. M. M., & Salman, S. A. Groundwater Quality Evaluation Using Hydrogeochemical and GIS Techniques in the Southwest Part of Sohag, Egypt. *The Iraqi Geological Journal.* 2022, 93-104. <https://doi.org/10.46717/igj.55.2A.7Ms-2022-07-23>
- [107] Gaikwad, S. K., Kadam, A. K., Ramgir, R. R., Kashikar, A. S., Wagh, V. M., Kandekar, A. M., & Kamble, K. D. Assessment of the groundwater geochemistry from a part of west coast of India using statistical methods and water quality index. *Hydro Research.* 2020, 3, 48-60. <https://doi.org/10.1016/j.hydres.2020.04.001>
- [108] Siban, M. & Zewd, I. The effects of alkalinity on physical and chemical properties of soil, *Journal of Plant Biology and Agricultural Sciences.* 2021, 3, 1-5. <https://doi.org/10.3626/GJAST/140>

- [109] Davis, J. G., Waskom, R. M. & Bauder, T. A. Managing Sodic Soils [Fact Sheet No. 0.504]. Mesa, CO: Colorado State University Extension. 2003, Available at: <https://extension.colostate.edu/topic-areas/agriculture/managing-sodic-soils-0-504/>
- [110] Garcia, R. New Mexico Integrated Cropping Systems and Water Management Handbook [AGRO-76]. Washington, DC: U.S. Department of Agriculture Natural Resources Conservation Service. 2014, Available at: https://www.nrcs.usda.gov/wps/portal/nrcs/detail/nm/technical/?cid%4nracs144p2_068965
- [111] Zhou, H., Shi, H., Yang, Y., Feng, X., Chen, X., Xiao, F. & Guo, Y. Insights into plant salt stress signalling and tolerance, *Journal of Genetics and Genomics*. 2024, 51(1), 16-34. <https://doi.org/10.1016/j.jgg.2023.08.007>
- [112] Abadi, H. T., Alemayehu, T., & Berhe, B. A. Assessing the suitability of water for irrigation purposes using irrigation water quality indices in the Irob catchment, Tigray, Northern Ethiopia. *Water Quality Research Journal*. 2025, 60(1), 177-195. <https://doi.org/10.2166/wqrj.2024.055>
- [113] Wilcox, L. V., 1955. Classification and use of irrigation waters, USDA, circular 969. DC, USA: Washington.
- [114] Selvakumar, S., Chandrasekar, N., Kumar, G. Hydrogeochemical characteristics and groundwater contamination in the rapid urban development areas of Coimbatore, India. *Water Resources and Industry*. 2017, 17, 26-33. <https://doi.org/10.1016/j.wri.2017.02.002>
- [115] Chitsazan, M., Aghazadeh, N., Mirzaee, Y., Golestan, Y., Mo-savi, S. Hydrochemical characteristics and quality assessment of urban groundwater in Urmia City, NW Iran. *Water Science and Technology: Water Supply*. 2017, 17(5), 1410-1425. <https://doi.org/10.2166/ws.2017.039>
- [116] Richards, L. A. Diagnosis and Improvement of Saline and Alkali Soils, U. S. Department of Agriculture Handbook. 1954, Vol. 60, Washington D. C., USA. 160 p.
- [117] Ravikumar, P., Somashekar, R. K., Angami, M. Hydrochemistry and evaluation of groundwater suitability for irrigation and drinking purposes in the Markandeya River basin, Belgaum District, Karnataka State, India. *Environmental monitoring and assessment*. 2011, 173(1), 459-487. <https://doi.org/10.1007/s10661-010-1399-2>
- [118] Hussain, Y., Ullah, S. F., Hussain, M. B. et al. Modelling the vulnerability of groundwater to contamination in an unconfined alluvial aquifer in Pakistan. *Environ Earth Sci*. 2017, 76, 84 <https://doi.org/10.1007/s12665-017-6391-5>
- [119] Neina, D. The role of soil pH in plant nutrition and soil remediation. *Applied and environmental soil science*. 2019, (1), 5794869. <https://onlinelibrary.wiley.com/journal/9248>
- [120] Doneen, L. D. Water Quality for Irrigated Agriculture. In: Poljakoff-Mayber, A., Gale, J. (eds) *Plants in Saline Environments*. Ecological Studies. 1975, vol 15. Springer, Berlin, Heidelberg. https://doi.org/10.1007/978-3-642-80929-3_5
- [121] Brown RM, McClelland NI, Deininger RA, O'Connor MF. A water quality index—crashing the psychological barrier. In *Indicators of Environmental Quality: Proceedings of a symposium held during the AAAS meeting in Philadelphia, Pennsylvania, 1972*, pp173-182. Springer US.
- [122] Chatterjee C, Raziuddin M. Determination of water quality index (WQI) of a degraded river in Asansol industrial area (West Bengal) *Ecology of polluted water*, 2002, Vol. II. Arvind Kumar published by Kul Bushan Nangia. pp. 885-897.
- [123] Aher DN, Kele VD, Malwade KD, Shelke MD. Lake water quality indexing to identify suitable sites for household utility: a case study Jambhulwadi Lake; Pune (MS). *International Journal of Engineering Research and Applications*, 2016, 6(5), 16-21.